Photocatalytic Amidation and Esterification with Perfluoroalkyl Iodide

Yelan Xiao, Yuen-Kiu Chun, Shun-Cheung Cheng, Chi-On Ng, Man-Kit Tse, Elva Ngai-Yu Lei, Ruoyang Liu and Chi-Chiu Ko*

Department of Chemistry, City University of Hong Kong, Tat Chee Avenue, Kowloon Tong, Hong Kong, China

Email: vinccko@cityu.edu.hk

Electronic Supplementary Information

Contents

1. Experimental Section

Materials and Reagents

All starting materials and solvents were purchased from commercial suppliers and used without further purification. Rhenium(I) complex, *cis,cis*-[$Re(CO)_2(CNC_6H_4Cl\text{-}4)_2(bpy)$]Br (**2**), was synthesized according to our previously published procedure (Scheme S1).[1] Iridium(III) complexes, *fac*-[$Ir(ppy)_3$] (**1**), {[$Ir(ppy)_2bpy$]PF_6} (**3**), and {[$Ir(dFppy)_2bpy$]PF_6} (**4**), were prepared according to the procedures reported in the literatures (Scheme S1).[2]

Physical Measurements and Instrumentation

^1H, ^{19}F and $^{13}C\{^1H\}$ NMR spectra were recorded on Bruker AV400 NMR and Bruker AV600 NMR spectrometers. The chemical shifts (δ, ppm) of ^1H and $^{13}C\{^1H\}$ NMR signals were reported relative to tetramethylsilane (Me_4Si) at 0 ppm, and the chemical shifts (δ, ppm) of ^{19}F NMR signals were reported relative to fluorobenzene (C_6H_5F) at −113.15 ppm. Multiplicities are abbreviated as follows: singlet (s), doublet (d), triplet (t), quartet (q), doublet-doublet (dd), multiplet (m). IR spectra were obtained from KBr disc by using a Perkin-Elmer Spectrum 100 FT-IR spectrophotometer. All ESI high resolution mass spectra (HRMS) for perfluoroalkyl amides products were recorded on Qstar elite hybrid LC/MS/MS system. All EI high resolution mass spectra (HRMS) for the perfluoroalkyl esters products were recorded on a Thermo Scientific DFS high-resolution magnetic sector mass spectrometer. Conversion was monitored by thin layer chromatography (TLC) using Merck TLC silica gel 60 F254, and gas chromatography-flame ionization detector (GC-FID), gas chromatography-mass spectrometry (GC-MS) using Agilent 7890A fitted with a DB-5MS UI column (30m, 0.25 mm, 0.25 um film) for FID analysis, and a HP 5973 fitted with a HP-5MS column (30m, 0.25 mm, 0.25 um film)

for MS analysis. 1,2-Dichlorobenzene was used as the internal standard for GC-FID analysis. GC-FID methods: 1 μL sample solution was injected in a pulse split mode (50:1) into GC-FID system consisting of an Agilent 6890 (Agilent Inc, Palo Alto, CA, USA) gas chromatography, Agilent 7890A autosampler. Compounds were visualized by UV light at 254 nm and by dipping the plates in the solvent of n-hexane or the mixed solvent of n-hexane/dichloromethane. All products were separated on column chromatography loaded with silica gel (100-200 mesh).

Luminescence lifetimes were measured on an Edinburgh Instrument LP920-KS Laser Flash Photolysis Spectrometer using the third harmonic output (355 nm; 6−8ns FWHM pulse width) of a Spectra-Physics Quanta-Ray Q-switched LAB-150 pulsed Nd:YAG laser (10 Hz) as the excitation source. Emission quenching experiments were carried out in solutions of a fix concentration of the luminescent complex, *fac*-[Ir(ppy)$_3$] (1.92×10^{-5} M), with a quencher of different concentrations, which were rigorously degassed on a high-vacuum line in a two-compartment cell with no less than four successive freeze pump-thaw cycles. With the emission lifetimes obtained from these experiments, the bimolecular quenching rate constants were determined using the Stern-Volmer equation:

$$\tau_0/\tau = 1 + k_q\tau_0[Q]$$

where k_q is bimolecular quenching rate constant;

τ_0 and τ are emission lifetime in the absence and presence of quencher, respectively;

[Q] is quencher concentration in mol dm^{-3}

Synthetic procedure for Photocatalysts

The synthetic routes for photocatalysts **1** – **4** are summarized in Scheme S1.[1-2] The detailed synthetic procedures and characterization of these photocatalysts are described below.

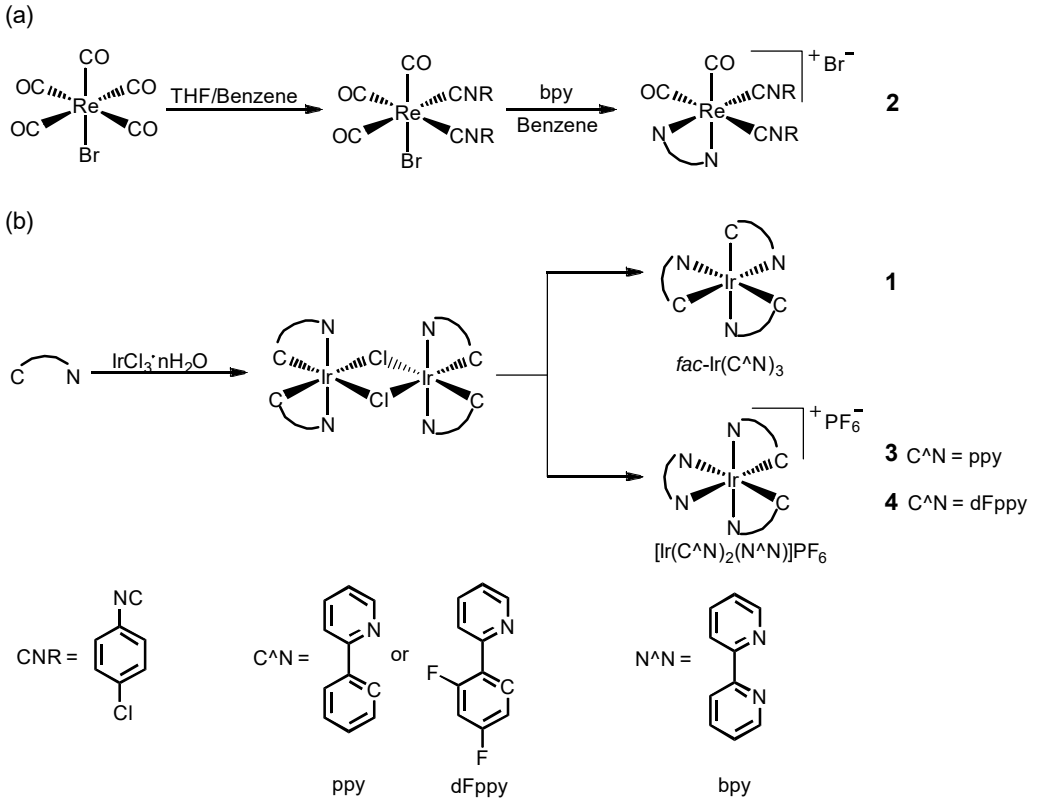

Scheme S1. Synthetic routes for (a) **2** and (b) **1, 3-4**

***fac*-[Ir(ppy)$_3$] (1):** Iridium(III) trichloride hydrate (388 mg, 1.30 mmol) and 2-phenylpyridine (760 mg, 4.90 mmol) were dissolved in a solvent mixture of 2-ethoxylethanol (3 mL) and water (1 mL). The resulting solution was refluxed for 24 hours under argon atmosphere. After that, the precipitate was collected and washed with ethanol (40 mL) and acetone (40 mL). This precipitate was re-dissolved in dichloromethane (50 mL). After removal of the solvent under reduced pressure, a yellow precipitate of [Ir(ppy)$_2$Cl]$_2$ was obtained and used for the subsequent reaction without further purification.

A solution of [Ir(ppy)$_2$Cl]$_2$ (128 mg, 0.12 mmol), ppy (93 mg, 0.60 mmol), and AgOTf (61 mg, 0.24 mmol) in 2-ethoxylethanol (20 mL) was refluxed overnight. Thereafter, the reaction mixture was cooled to room temperature, 50 mL DI water was added and the crude product was extracted thrice with dichloromethane (50 mL). The combined

dichloromethane extracts were dried over anhydrous $MgSO_4$. After removal of the solvent under reduced pressure, the residue was purified by column chromatography on silica gel using dichloromethane-*n*-hexane (2:1, v/v) as eluent. The analytically pure complex **1** as yellow precipitate was obtained after removal of the solvent under reduced pressure and dried in vacuum. Yield: 56 %; ^{1}H NMR (400 MHz, $CDCl_3$): δ 7.88 (d, J = 8.2 Hz, 3H), 7.66 (d, J = 7.9 Hz, 3H), 7.59 (t, J = 7.7 Hz, 3H), 7.53 (d, J = 5.6 Hz, 3H), 6.90 (m, 6H), 6.84 (d, J = 6.0 Hz, 6H). Positive-ion ESI-MS: *m/z* 655.2 $[M+H]^+$; IR (KBr disc): 3035, 2925, 1650, 1599, 1580, 1560, 1472, 1413, 1261, 1161, 1085, 1031, 752, 733 cm^{-1}; Elemental analyses calcd (%) for $C_{33}H_{24}N_3Ir$: C 60.53, H 3.69, N 6.42 ; found: C 60.47, H 4.13 , N 6.18.

***cis,cis*-{[Re(CO)$_2$(CNC$_6$H$_4$Cl-4)$_2$(bpy)]Br} (2):** A solution of $[Re(CO)_5(Br)]$ (600 mg, 1.48 mmol) and CNC_6H_4Cl-4 (426 mg, 3.10 mmol) in THF-benzene (1:1, v/v, 120 mL) was refluxed overnight. After removal of the solvent under reduced pressure, the residue was purified by column chromatography on silica gel using dichloromethane-petroleum ether (1:1, v/v) as eluent. The pure product of *fac*-$\{[Re(CO)_3(CNC_6H_4Cl\text{-}4)_2](Br)\}$ was collected after removal of solvent and used for the subsequent photo-ligand substitution reaction.

A benzene solution (30 mL) of *fac*-$\{[Re(CO)_3(C_6H_4Cl\text{-}4)_2](Br)\}$ (100 mg, 0.16 mmol) and bpy (100 mg, 0.64 mmol) was irradiated with UV light (λ=254 nm) for 3 hours at room temperature with Pen-Ray mercury lamp (11SC-1) in a water-cooled quartz jacket. After removal of the solvent under reduced pressure, the residue was purified on silica gel column chromatography using dichloromethane-methanol (9:1, v/v) as eluent. The pure complex **2** was obtained after removal of the solvent and dried in vacuo. Yield: 71 %; ^{1}H NMR (400 MHz, $CDCl_3$): δ 9.43 (d, J = 9.3 Hz, 1H), 9.38 (d, J = 8.3 Hz, 1H), 9.08 (t,

J = 7.0 Hz, 2H), 8.39 (t, *J* = 7.5 Hz, 1H), 8.31 (t, *J* = 8.2 Hz, 1H), 7.75 (t, *J* = 6.8 Hz, 1H), 7.58 (m, 1H), 7.44 (q, *J* = 8.5 Hz, 5H), 7.35 (d, *J* = 7.4 Hz, 3H). Positive-ion ESI-MS: *m/z* 673.2 $[M–Br]^+$; IR (KBr disc): 2162, 2094, 1967, 1909, 1638, 1604, 1484, 1443, 1383, 1092, 1008, 830, 768 cm^{-1}; Elemental analyses calcd (%) for $C_{26}H_{16}N_4O_2Cl_2ReBr·0.5H_2O$: C 40.96, H 2.25, N 7.35; found: C 40.50, H 2.61, N 7.35.

***cis,cis*-{[Ir(ppy)$_2$(bpy)]PF$_6$} (3):** A solution of $[Ir(ppy)_2Cl]_2$ (107 mg, 0.10 mmol) and bpy (39 mg, 0.25 mmol) in dichloromethane-methanol (2:1, v/v, 12 mL) was refluxed for 6 hours. After cooling, 10-fold excess of NH_4PF_6 was added into the mixture and stirred for 30 min to commence precipitation. The crude product was collected by filtration. It was purified by column chromatography on silica gel using dichloromethane-methanol (10:1, v/v) as eluent. The analytically pure complex **3** was obtained as yellow powder after removal of the solvent under reduced pressure and dried in vacuo. Yield: 80 %; ^1H NMR (400 MHz, $CDCl_3$): δ 8.68 (d, *J* = 8.1 Hz, 1H), 8.14 (t, *J* = 8.1 Hz, 1H), 7.93 (t, *J* = 7.6 Hz, 2H), 7.76 (t, *J* = 7.8 Hz, 1H), 7.69 (d, *J* = 8.3 Hz, 1H), 7.51 (d, *J* = 6.3 Hz, 1H), 7.42 (m, 1H), 7.05 (t, *J* = 7.2 Hz, 2H), 6.93 (t, *J* = 7.3 Hz, 1H), 6.30 (d, *J* = 8.1 Hz, 1H). Positive-ion ESI-MS: *m/z* 657.3 $[M–PF_6]^+$; IR (KBr disc):3040, 1608, 1583, 1479, 1446, 1423, 1315, 1269, 1163, 1064, 1031, 841, 762, 757, 739, 731, 558 cm^{-1}; Elemental analyses calcd (%) for $C_{32}H_{24}N_4IrPF_6·0.5CH_2Cl_2$: C 46.24, H 2.98, N 6.64; found: C 46.79, H 3.16, N 6.85.

***cis,cis*-{[Ir(dFppy)$_2$bpy]PF$_6$} (4):** A solution mixture of $[Ir(dFppy)_2Cl]_2$ (219 mg, 0.18 mmol) and bpy (65 mg, 0.42 mmol) in 1,2-ethanediol (15 mL) was refluxed overnight. After cooling to room temperature, 10-fold excess NH_4PF_6 was added and stirred for 30 min. The crude product was collected by filtration. It was purified by column

chromatography on silica gel using dichloromethane-methanol (10:1, v/v) as eluent. The pure product of **4** was collected after removal of the solvent and dried in vacuum. Yield: 61 % ; ^{1}H NMR (400 MHz, $CDCl_3$): δ 8.71 (d, J = 8.1 Hz, 2H), 8.33 (d, J = 7.0 Hz, 2H), 8.21 (t, J = 8.7 Hz, 2H), 7.95 (d, J = 4.4 Hz, 2H), 7.83 (t, J = 7.7 Hz, 2H), 7.50 (m, 4H), 7.13 - 7.06 (m, 2H), 6.59 (m, 2H), 5.69 (dd, J = 8.2, 2.3 Hz, 2H). ^{19}F NMR (376 MHz, $CDCl_3$): δ – 72.11 (s, 1F), – 74.00 (s, 1F), – 105.22 (d, J = 10.9 Hz, 1F), – 108.28 (d, J = 11.0 Hz, 1F). Positive-ion ESI-MS: *m/z* 729.5 $[M–PF_6]^+$; IR (KBr disc): 3087, 1605, 1575, 1560, 1479, 1448, 1430, 1406, 1314, 1295, 1248, 1166, 1117, 1106, 1044, 990, 843, 786, 761, 558, 527 cm^{-1}; Elemental analyses calcd (%) for $C_{32}H_{20}N_4F_4IrPF_6 \cdot 0.5CH_2Cl_2$: C 42.61, H 2.31, N 6.12; found: C 42.57, H 2.50, N 6.17.

General synthetic procedures for photocatalytic amidation and esterification with perfluoroalkyl iodide

General Procedure for photocatalytic amidation. A solution of perfluoroalkyl halides (0.427 mmol, 6.67 mM), amines (0.854 mmol, 2.0 equiv., 13.34 mM) and 1 mol % photocatalysts (4.27 μmol, 1 mol%) in acetonitrile (64 mL) was transferred to reaction tubes. The solution was irradiated for 10 hours in a merry-go-round photoreactor equipped with white-light LEDs as the excitation source. After irradiation and removal of solvent under reduced pressure, the crude product was collected. The analytically pure products can be obtained after purification with column chromatography on silica gel using dichloromethane-hexane (2:3, v/v) as eluent.

General Procedure for photocatalytic esterication. The photocatalytic esterification reactions were performed based on procedures similar to those for amide except alcohols

(2.135 mmol, 33.35 mM) was used in place of amides. The pure products can be obtained after purification with column chromatography on silica gel using dichloromethane-hexane (2:3, v/v) for amides or dichloromethane-hexane (1:4, v/v) for esters as eluent. All purified perfluoroalkyl amides and esters were characterized by ^{1}H NMR, ^{19}F NMR, $^{13}C\{^{1}H\}$ NMR, IR spectroscopy and high resolution mass spectrometry (HRMS). The reaction yields of perfluoroalkyl amides were determined by gas chromatography-flame ionization detector (GC-FID). The reaction yields of perfluoroalkyl esters were determined by ^{19}F NMR using fluorobenzene as the internal standard.

2. Characterization of Perfluoroalkyl Amides and Esters

Characterization of Perfluoroalkyl Amides

1a

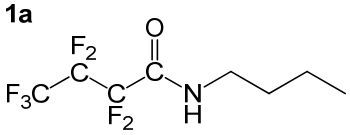

N-butyl perfluorobutanamide (**1a**): colorless oil. ^{1}H NMR (600 MHz, $CDCl_3$): δ 6.32 (s, 1H), 3.40 (dd, J = 13.5, 6.8 Hz, 2H), 1.57 (m, 2H), 1.37 (m, 2H), 0.95 (t, J = 7.4 Hz, 3H); ^{19}F NMR (565 MHz, $CDCl_3$): δ –81.6 (t, J = 8.7 Hz, 3F), –121.8 (q, J = 8.7 Hz, 2F), –128.0 (s, 2F). ^{13}C{^{1}H} NMR (151 MHz, $CDCl_3$): δ 157.5 (t, J = 25.7 Hz), 117.5 (qt, J = 287.6, 33.6 Hz), 108.3 (m), 39.9 (s), 30.9 (s), 19.7 (s), 13.4 (s). IR: 3319, 2965, 2938, 2878, 1704 (C=O), 1549, 1462, 1353, 1232, 1219, 1125 cm^{-1}. HRMS (ESI) *m/z* calculated for $C_8H_9F_7NO$ [M–H]$^-$: 268.0572, found 268.0594.

1b

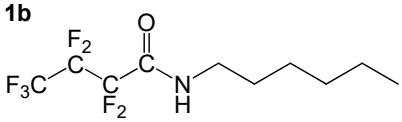

N-hexyl perfluorobutanamide (**1b**): white solid. ^{1}H NMR (600 MHz, $CDCl_3$): δ 6.32 (s, 1H), 3.39 (dd, J = 13.5, 7.3 Hz, 2H), 1.58 (m, 2H), 1.33 (m, 6H), 0.89 (t, J = 6.8 Hz, 3H). ^{19}F NMR (565 MHz, $CDCl_3$): δ –81.6 (t, J = 8.7 Hz, 3F), –121.8 (q, J = 8.7 Hz, 2F), –128.0 (s, 2F). ^{13}C{^{1}H} NMR (151 MHz, $CDCl_3$): δ 157.6 (t, J = 25.7 Hz), 117.5 (qt, J = 287.6, 33.6 Hz), 108.4 (m), 40.2 (s), 31.2 (s), 28.8 (s), 26.2 (s), 22.3 (s), 13.7 (s). IR: 3329, 2962, 2936, 2865, 1703 (C=O), 1549, 1469, 1446, 1353, 1232, 1219, 1190, 1164, 1124 cm^{-1}. HRMS (ESI) *m/z* calculated for $C_{10}H_{13}F_7NO$ [M–H]$^-$: 296.0885, found 296.0846.

1c

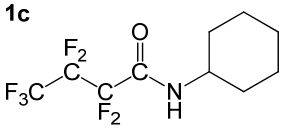

N-cyclohexyl perfluorobutanamide (**1c**): white solid. ^{1}H NMR (600 MHz, $CDCl_3$): δ 6.14 (s, 1H), 3.85 (m, 1H), 1.97 (m, 2H), 1.75 (m, 2H), 1.65 (m, 1H), 1.40 (m, 2H), 1.23 (m, 3H). ^{19}F NMR (565 MHz, $CDCl_3$): δ –81.6 (t, J = 8.6 Hz, 3F), –121.9 (q, J = 8.6 Hz, 2F), –128.1 (s, 2F). ^{13}C{^{1}H} NMR (151 MHz, $CDCl_3$): δ 156.5 (t, J = 25.4 Hz), 117.5 (qt, J = 287.8, 33.5 Hz), 108.2 (m), 49.44 (s), 32.4 (s), 25.2 (s), 24.5 (s). IR: 3314, 3090, 2948, 2861, 1695 (C=O), 1555, 1454, 1383, 1357, 1353, 1326, 1297, 1282, 1244, 1217, 1176 cm^{-1}. HRMS (ESI) *m/z* calculated for $C_{10}H_{11}F_7NO$ [M–H]$^-$: 294.0729, found 294.0703.

1d

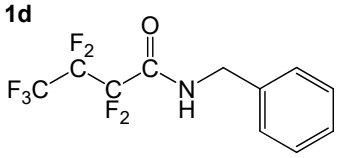

N-benzyl perfluorobutanamide (**1d**): white solid. ^{1}H NMR (600 MHz, $CDCl_3$): δ 7.38 (t, J = 7.0 Hz, 2H), 7.34 (t, 1H), 7.29 (d, J = 7.0 Hz, 2H), 6.60 (s, 1H), 4.57 (s, 1H,), 4.56 (s, 1H). ^{19}F NMR (565 MHz, $CDCl_3$): δ –81.5 (t, J = 8.8 Hz, 3F), –121.6 (q, J = 8.8 Hz, 2F), –127.9 (s, 2F). ^{13}C{^{1}H} NMR (151 MHz, $CDCl_3$): δ 157.5 (t, J = 26.0 Hz), 135.9 (s), 129.0 (s), 128.3 (s), 127.8 (s), 117.5 (qt, J = 287.9, 33.6 Hz), 117.5 (m), 44.1 (s). IR: 3315, 3086, 3068, 3034, 2952, 1690 (C=O), 1552, 1453, 1363, 1312, 1221, 1176, 1150 cm^{-1}. HRMS (ESI) *m/z* calculated for $C_{11}H_7F_7NO$ [M–H]$^-$: 302.0416, found 302.0415.

1e

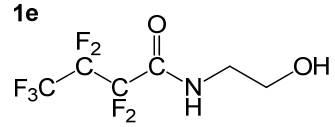

N-(2-hydroxyethyl perfluorobutanamide (**1e**): white solid. ^{1}H NMR (600 MHz, $CDCl_3$): δ 6.83 (s, 1H), 3.82 (t, J = 5.0 Hz, 2H), 3.58 (dd, J = 10.5, 5.0 Hz, 2H). ^{19}F NMR (565 MHz, $CDCl_3$): δ –81.6 (t, J = 8.8 Hz, 3F), –121.7 (q, J = 8.8 Hz, 2F), –128.0 (s, 2F).

$^{13}C\{^{1}H\}$ NMR (151 MHz, $CDCl_3$): δ 158.0 (t, J= 26.0 Hz), 117.4 (qt, J = 287.4, 33.3 Hz), 108.3 (m), 60.7 (s), 42.2 (s). IR: 3319, 3088, 2995, 2959, 2894, 1701 (C=O), 1555, 1445, 1358, 1303, 1232, 1218, 1178, 1154, 1123, 1058, 1043 cm^{-1}. HRMS (ESI) *m/z* calculated for $C_6H_5F_7NO_2$ $[M–H]^–$: 256.0208, found 256.0168.

1f

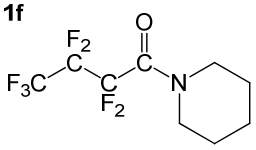

1-Piperidinyl perfluorobutanamide (**1f**): white solid. ^{1}H NMR (600 MHz, CDCl3): δ 3.64 (m, 2H), 3.59 (m, 2H), 1.70 (m, 2H), 1.65 (m, 4H). ^{19}F NMR (565 MHz, $CDCl_3$): δ –80.7 (t, J = 9.4 Hz, 3F), –112.6 (q, J = 9.4 Hz, 2F), –126.6 (s, 2F). $^{13}C\{^{1}H\}$ NMR (151 MHz, $CDCl_3$): δ 156.1 (t, J = 25.0 Hz), 117.7 (qt, J = 288.0, 33.8 Hz), 109.4 (m), 46.9 (s), 45.1 (s), 26.4 (s), 25.5 (s), 24.20 (s). IR: 2945, 2932, 2863, 1685 (C=O), 1603, 1474, 1449, 1349, 1232, 1212, 1173, 1131, 1118 cm^{-1}. HRMS (ESI) *m/z* calculated for $C_9H_{11}F_7NO$ $[M+H]^+$: 282.0729, found 282.0723.

1g

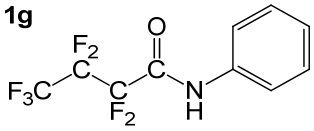

N-phenyl perfluorobutanamide (**1g**): white solid. ^{1}H NMR (600 MHz, $CDCl_3$): δ 7.88 (s, 1H), 7.57 (d, J = 7.7 Hz, 2H), 7.41 (t, J = 7.7 Hz, 2H), 7.27 (t, J = 7.7 Hz, 1H). ^{19}F NMR (565 MHz, $CDCl_3$): δ –81.5 (t, J = 8.9 Hz, 3F), –121.3 (q, J = 8.9 Hz, 2F), –127.7 (s, 2F). $^{13}C\{^{1}H\}$ NMR (151 MHz, $CDCl_3$): δ 155.1 (t, J = 25.6 Hz), 135.1 (s), 129.4 (s), 126.5 (s), 120.5 (s), 117.5 (qt, J = 287.7, 33.3 Hz), 108.6 (m). IR: 3320, 1699 (C=O), 1602, 1545, 1450, 1357, 1234, 1224, 1199, 1167, 1149, 1127, 752 cm^{-1}. HRMS (ESI) *m/z* calculated for $C_{10}H_5F_7NO$ $[M–H]^–$: 288.0259, found 288.0276.

1h

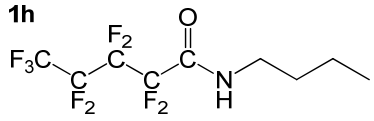

N-butyl perfluoropentanamide (**1h**): colorless oil. ^{1}H NMR (600 MHz, $CDCl_3$): δ 6.32 (s, 1H), 3.40 (dd, J = 13.5, 7.4 Hz, 2H), 1.58 (q, J = 7.4 Hz, 2H), 1.38 (q, J = 7.4 Hz, 2H), 0.95 (t, J = 7.4 Hz, 3H). ^{19}F NMR (565 MHz, $CDCl_3$): δ –80.9 (t, J = 9.7 Hz, 3F), –120.0 (t, J = 9.7 Hz, 2F), –123.5 (m, 2F), –125.9 (m, 2F). ^{13}C{^{1}H} NMR (151 MHz, $CDCl_3$): δ 157.4 (t, J = 25.6 Hz), 117.3 (qt, J = 288.3, 33.1 Hz), 109.5 (m), 39.9 (s), 31.0 (s), 19.8 (s), 13.5 (s). IR: 3459, 3331, 3092, 2910, 2941, 2878, 1704 (C=O), 1549, 1239, 1211, 1140 cm^{-1}. HRMS (ESI) *m/z* calculated for $C_9H_9F_9NO$ $[M–H]^-$: 318.0540, found 318.0554.

1i

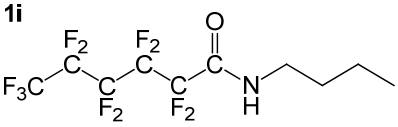

N-butyl perfluorohexanamide (**1i**): colorless oil. ^{1}H NMR (600 MHz, $CDCl_3$): δ 6.31 (s, 1H), 3.40 (dd, J = 13.4, 7.3 Hz, 2H), 1.58 (d, J = 7.3 Hz, 2H), 1.38 (q, J = 7.4 Hz, 2H), 0.95 (t, J = 7.4 Hz, 3H). ^{19}F NMR (565 MHz, $CDCl_3$): δ –81.7 (t, J = 9.8 Hz, 3F), –120.8 (t, J = 9.8 Hz, 2F), –123.5 (m, 2F), –123.7 (m, 2F), –127.2 (m, 2F). ^{13}C{^{1}H} NMR (151 MHz, $CDCl_3$): δ 157.5 (t, J = 25.7 Hz), 117.2 (qt, J = 288.5, 33.1 Hz), 109.8 (m), 39.93 (s), 30.92 (s), 19.76 (s), 13.45 (s). IR: 3546, 3468, 3415, 2969, 2943, 2880, 1704 (C=O), 1619, 1552, 1240, 1205, 1141 cm^{-1}. HRMS (ESI) *m/z* calculated for $C_{10}H_9F_{11}NO$ $[M–H]^-$: 368.0508, found 368.0523.

Characterization of Perfluoroalkyl Esters

2a

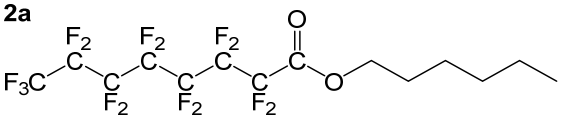

Hexyl perfluorooctanoate **(2a)**: colorless oil. ^{1}H NMR (600 MHz, $CDCl_3$): δ 4.38 (m, 2H), 1.74 (m, 2H), 1.38 (m, 2H), 1.31 (m, 4H), 0.90 (m, 3H). ^{19}F NMR (565 MHz, $CDCl_3$): δ –80.79 (t, J = 9.6 Hz, 3F), –118.52 (t, J = 11.3Hz, 2F), –121.71 (s, 2F), –122.05 (s, 2F), –122.71 (dd, J = 22.1, 8.4 Hz, 4F), –126.15 (t, J = 17.8Hz, 2F). ^{13}C{^{1}H} NMR (151 MHz, $CDCl_3$): δ 158.56 (t, J = 29.3 Hz), 68.83 (s), 31.30 (s), 28.21 (s), 25.26 (s), 22.53 (s), 13.89 (s). IR (KBr disc): 2965, 2937, 2865, 1785 (C=O), 1470, 1331, 1244, 1211, 1149 cm^{-1}. HRMS (EI) *m/z* calculated for $C_{14}H_{13}F_{15}O_2$: 498.0676, found 498.0603.

2b

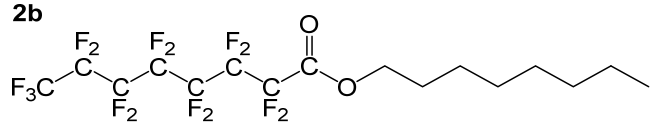

Octyl perfluorooctanoate **(2b)**: colorless oil. ^{1}H NMR (600 MHz, $CDCl_3$): δ 4.37 (t, J = 6.7 Hz, 2H), 1.75 (m, 2H), 1.35 (m, 10H), 0.89 (t, 3H). ^{19}F NMR (565 MHz, $CDCl_3$): δ –80.79 (t, J = 9.7 Hz, 3F), –118.52 (t, J = 11.9 Hz, 2F), –121.71 (s, 2F), –122.05 (s, 2F), –122.72 (m, 4F), –126.15 (dd, J = 13.7, 8.4 Hz, 2F). ^{13}C{^{1}H} NMR (151 MHz, $CDCl_3$): δ 158.50 (t, J = 29.3 Hz), 68.84 (s), 31.90 (s), 29.26 (s), 29.17 (s), 28.30 (s), 25.65 (s), 22.77 (s), 14.03 (s). IR (KBr disc): 2964, 2934, 2862, 1785 (C=O), 1470, 1331, 1243, 1211, 1150 cm^{-1}. HRMS (EI) *m/z* calculated for $C_{16}H_{17}F_{15}O_2$: 526.0989, found 526.0956.

2c

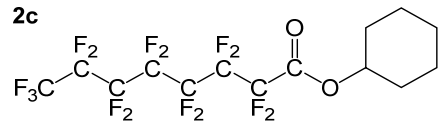

Cyclohexyl perfluorooctanoate **(2c)**: colorless oil. ^{1}H NMR (600 MHz, $CDCl_3$): δ 5.05 (m, 1H), 1.92 (m, 2H), 1.77 (m, 2H), 1.61 (m, 3H), 1.45 (m, 2Hs), 1.35 (m, 1H). ^{19}F NMR (565 MHz, $CDCl_3$): δ –80.78 (t, J = 9.2Hz, 3F), –118.64 (t, J = 12.0 Hz, 2F), –121.64 (s,

2F), −122.06 (s, 2F), −122.71 (m, 4F), −126.15 (t, J = 17.8 Hz, 2F). $^{13}C\{^{1}H\}$ NMR (151 MHz, $CDCl_3$): δ 157.92 (t, J = 29.2 Hz), 78.16 (s), 31.02 (s), 25.16 (s), 23.28 (s). IR (KBr disc): 2947, 2868, 1779 (C=O), 1455, 1333, 1309, 1243, 1209, 1149 cm^{-1}. HRMS (EI) *m/z* calculated for $C_{14}H_{11}F_{15}O_2$: 496.0519, found 496.0468.

2d

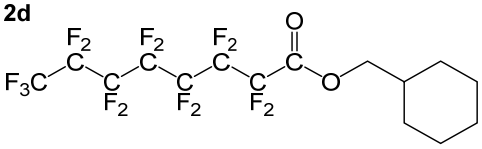

Cyclohexylmethyl perfluorooctanoate **(2d)**: colorless oil. ^{1}H NMR (600 MHz, $CDCl_3$): δ 4.18 (d, J = 6.1Hz, 2H), 1.74 (m, 5H), 1.28 (m, 4H), 1.02 (m, 2H). ^{19}F NMR (565 MHz, $CDCl_3$): δ −80.78 (t, J = 9.0Hz, 3F), −118.42 (t, J = 12.1Hz, 2F), −121.72 (s, 2F), −122.04 (s, 2F), −122.68 (m, 4F), −126.14 (m, 2F). $^{13}C\{^{1}H\}$ NMR (151 MHz, $CDCl_3$): δ 158.54 (t, J = 29.2 Hz), 73.52 (s), 36.89 (s), 29.27 (s), 26.21 (s), 25.56 (s). IR (KBr disc): 2933, 2860, 1784 (C=O), 1454, 1329, 1242, 1210, 1149 cm^{-1}. HRMS (EI) *m/z* calculated for $C_{15}H_{13}F_{15}O_2$: 510.0676, found 510.0696.

2e

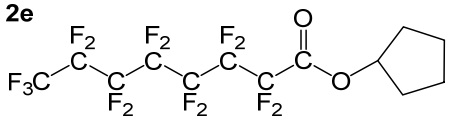

Cyclopentyl perfluorooctanoate **(2e)**: colorless oil. ^{1}H NMR (600 MHz, $CDCl_3$): δ 5.43 (m, 1H), 1.93 (m, 2H), 1.83 (m, 2H), 1.77 (m, 2H), 1.67 (m, 2H). ^{19}F NMR (565 MHz, $CDCl_3$): δ −80.79 (t, J = 9.7 Hz, 3F), −118.67 (t, J = 12.0 Hz, 2F), −121.68 (s, 2F), −122.07 (s, 2F), −122.73 (m, 4F), −126.15 (dd, J = 13.5, 8.6 Hz, 2F). $^{13}C\{^{1}H\}$ NMR (151 MHz, $CDCl_3$): δ 158.12 (t, J = 29.2 Hz), 82.69 (s), 32.55 (s), 23.51 (s). IR (KBr disc): 2978, 2885, 1781 (C=O), 1440, 1334, 1244, 1209, 1149 cm^{-1}. HRMS (EI) *m/z* calculated for $C_{13}H_9F_{15}O_2$: 482.0363, found 482.0345.

2f

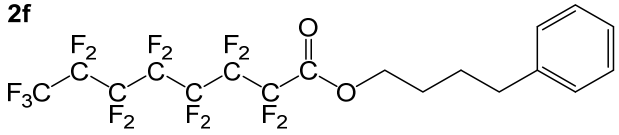

Phenylbutyl perfluorooctanoate **(2f)**: colorless oil. ^{1}H NMR (600 MHz, $CDCl_3$): δ 7.29 (m, 2H), 7.18 (m, 3H), 4.37 (dd, J = 7.8, 4.6 Hz, 2H), 2.65 (dd, J = 9.9, 4.6 Hz, 2H), 1.73 (m, 4H). ^{19}F NMR (565 MHz, $CDCl_3$): δ −80.77 (t, J = 9.7Hz, 3F), −118.48 (t, J = 12.0 Hz, 2F), −121.70 (s, 2F), −122.04 (s, 2F), −122.68 (dd, J = 34.5, 26.5 Hz, 4F), −126.14 (d, J = 8.1 Hz, 2F). ^{13}C{^{1}H} NMR (151 MHz, $CDCl_3$) δ 158.50 (t, J = 29.5 Hz), 141.58 (s), 128.55 (s), 128.45 (s), 126.15 (s), 68.52 (s), 35.29 (s), 27.76 (s), 27.29 (s). IR (KBr disc): 3030, 2930, 2862, 1782 (C=O), 1497, 1454, 1330, 1242, 1210, 1149 cm^{-1}. HRMS (EI) *m/z* calculated for $C_{18}H_{13}F_{15}O_2$: 546.0676, found 546.0665.

2g

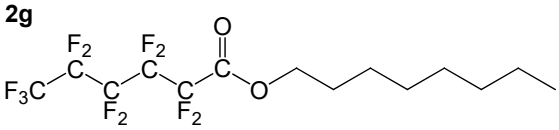

Octyl perfluorohexanoate **(2g)**: colorless oil. ^{1}H NMR (600 MHz, $CDCl_3$): δ 4.37 (t, J = 6.7Hz, 2H), 1.74 (m, 2H), 1.39 (m, 2H), 1.34 (m, 8H), 0.89 (t, J = 6.8 Hz, 3H). ^{19}F NMR (565 MHz, $CDCl_3$): δ −80.83 (t, J = 9.9 Hz, 3F), −118.58 (t, J = 12.2 Hz, 2F), −122.72 (d, J = 9.6 Hz, 2F), −122.95 (d, J = 9.0 Hz, 2F), −126.27 (m, 2F). ^{13}C{^{1}H} NMR (151 MHz, $CDCl_3$): δ 158.52 (t, J = 29.3 Hz), 68.83 (s), 31.82 (s), 29.17 (s), 29.08 (s), 28.23 (s), 25.57 (s), 22.71 (s), 14.07 (s). IR (KBr disc): 2962, 2931, 2861, 1785 (C=O), 1467, 1320, 1241, 1206, 1149 cm^{-1}. HRMS (EI) *m/z* calculated for $C_{14}H_{17}F_{11}O_2$: 426.1053, found 426.0996.

3. ESI-MS of Radical Trapping Experiment

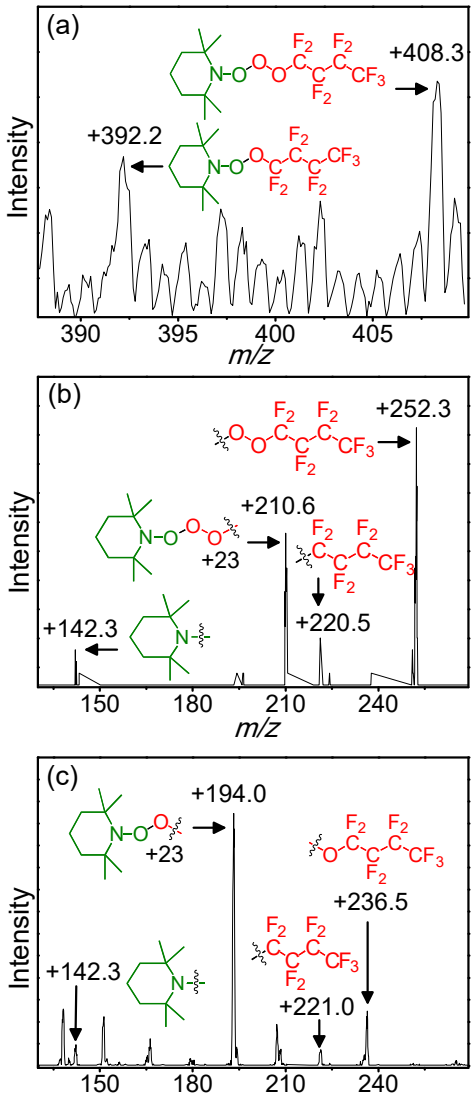

Figure S1. (a) ESI-mass spectrum of the reaction mixture between TEMPO radical (2.0 mole equivalents) and the solution of the photocatalytic reaction of perfluorobutyl iodide (6.67 mM), *n*-butyl amine (2.0 mole equivalents), *fac*-[Ir(ppy)$_3$] (1 mol %), air atmosphere, after 30-min photoexcitation. MS/MS mass spectra of the peaks at (b) $^+$ 408.3 (*m/z*) and (c) $^+$ 392.2 (*m/z*).

4. DFT Calculations

Computation Details

All the calculations were done using GAUSSIAN 09 package, version B.01.[3] The structures of the reactant complexes, transition states and product complexes of the photocatalytic reaction were optimized using density functional theory (DFT). The B3LYP functional[4] and a mixed basis set of 6-31+G(d) (for H, C, O and F) and LANL2DZ (for Ir and I) was employed.[5] Frequency analysis were done after optimizations to ensure the structures are at minimum (for products) and in a first-order saddle point (for transition states) of the potential energy surfaces. The solvent effects were taken account by the polarized continuum model with integral equation formulism (IEF-PCM).[6]

Cartesian Coordinates and Energies of the Optimized Structures

Table S1. Free energy changes (ΔG) and activation free energies ($\Delta G^{\ddagger}$) for the possible reactions of the catalytic cycle

Reaction[a]	ΔG(kcal/mol)	$\Delta G^{\ddagger}$(kcal/mol)
Step 1: $[Ir(ppy)_3]^{3*}+C_6FI \rightarrow [Ir(ppy)_3]^{+\bullet}+C_6F^{\bullet}+I^{-}$	−32.3	barrierless
Step 2: $C_6F^{\bullet} + O_2 \rightarrow C_6F{-}OO^{\bullet}$	−21.0	barrierless
Step 3a: $C_6FOO^{\bullet} + C_6FOO^{\bullet} \rightarrow (C_6FOO{-}OOC_6F)$	−7.9	+15.7
Step 4a: $(C_6FOOOOC_6F) \rightarrow 2C_6FO^{\bullet} + O_2$	−5.9	+21.4
Alternatively, Step 3b: $C_6FOO^{\bullet} + C_6F^{\bullet} \rightarrow (C_6FOO{-}C_6F)$	−60.1	+8.1
Step 4b: $(C_6FOOC_6F) \rightarrow 2C_6FO^{\bullet}$	+26.8	+41.9
Step 5: $C_6FO^{\bullet} + H_3CCN \rightarrow C_6FOH + {}^{\bullet}H_2CCN$	−22.7	+7.3
Alternatively, Step 5b: $C_6FO^{\bullet} + H_2O \rightarrow C_6FOH + OH^{\bullet}$	−1.4	+9.0
Step 6: $C_6FOH \rightarrow C_5FCOF + HF$ (with CH_3CN)	−2.5	+22.4
$C_6FOH \rightarrow C_5FCOF + HF$ (without CH_3CN)	−1.9	+42.7

[a]: For simplicity, $C_5F = CF_3(CF_2)_4-$ and $C_6F = CF_3(CF_2)_5-$

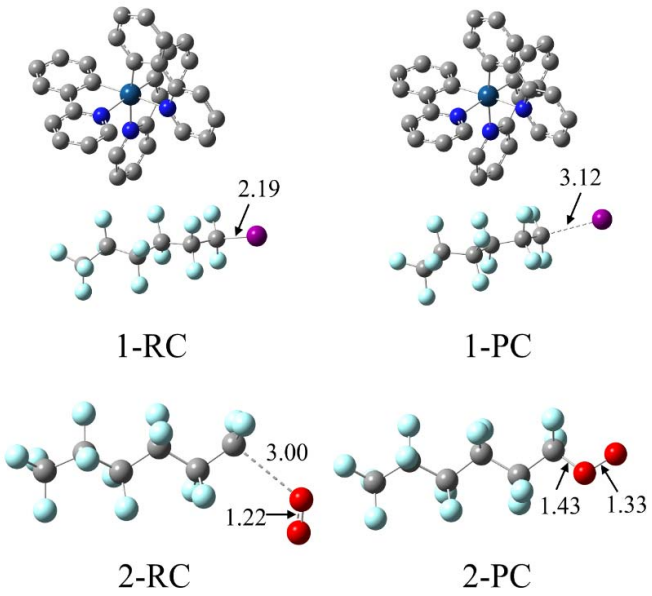

Figure S2. DFT optimized structures of the reactant and product complex for the steps 1 and 2 of the photocatalytic reaction mechanism.

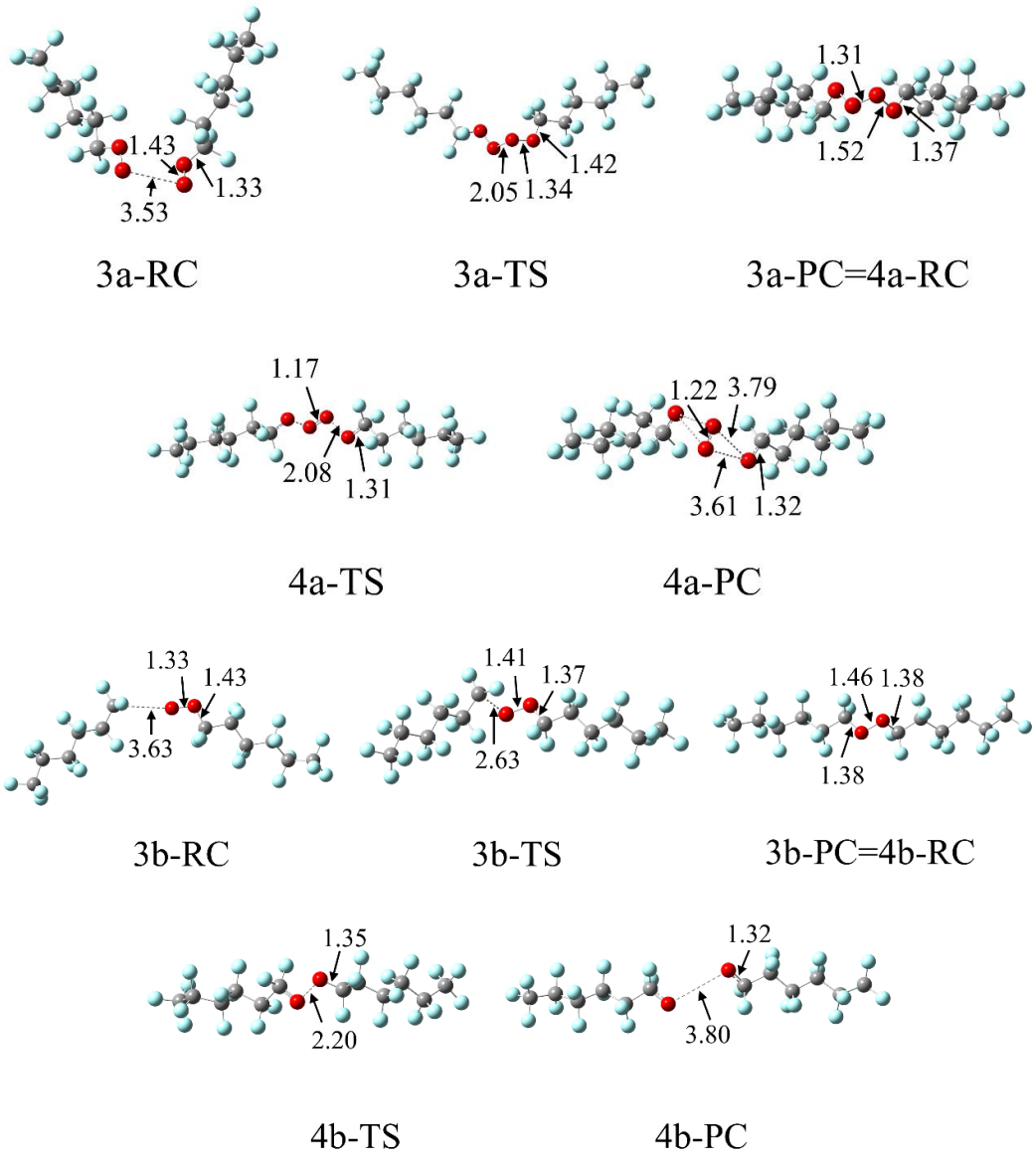

Figure S3. DFT optimized structures of the reactant and product complex for the steps 3a/b and 4a/b of the photocatalytic reaction mechanism.

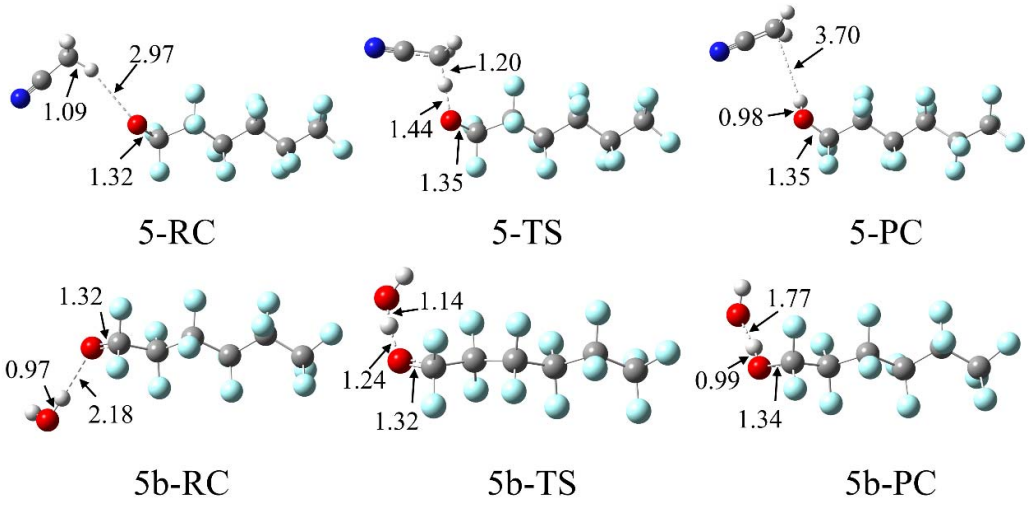

Figure S4. DFT optimized structures of the reactant and product complex for the steps 5 of the photocatalysis mechanism.

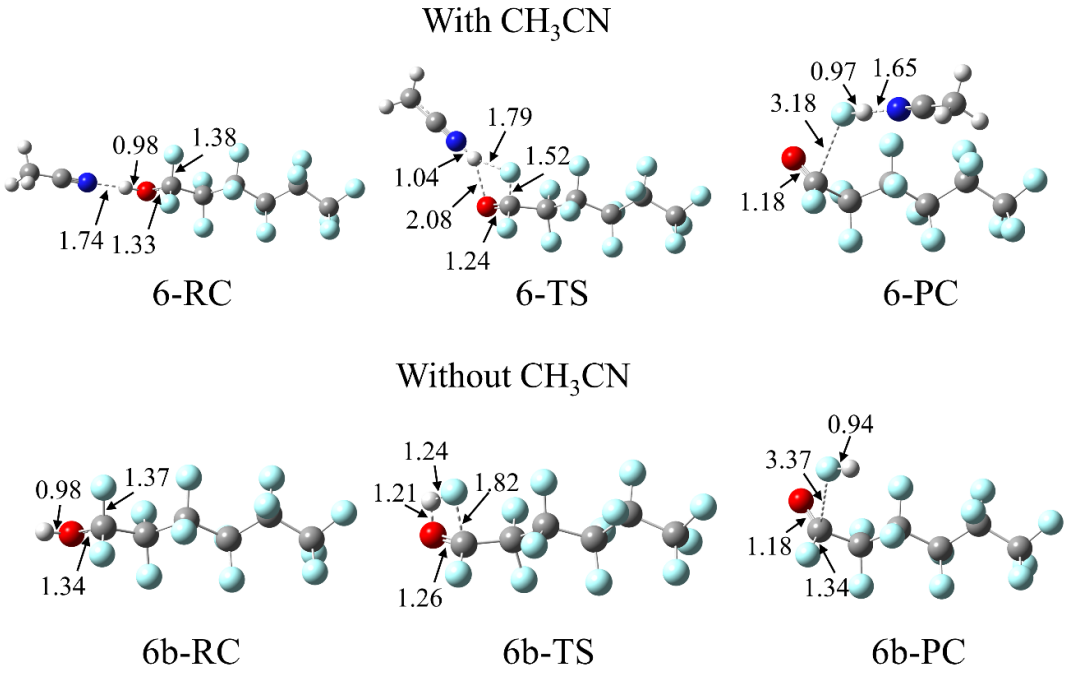

Figure S5. DFT optimized structures of the reactant and product complex for the steps 6 of the photocatalytic reaction mechanism.

Table S2. Total electronic energies (E), Zero-point energy (ZPE) corrections[a], Thermal corrections to Gibbs free energies[a], and Number of imaginary frequencies of the structures discussed in Figure S1-S4.

	Structure	E / Hartree	ZPE corr./ Hartree	Thermal corrections to G/ Hartree	No. of imaginary frequencies
1-RC	$[Ir(ppy)_3]^{3*}$ + C_6FI	-3078.96145900	0.551009	0.452462	0
1-PC	$[Ir(ppy)_3]^{+\bullet}$ + $C_6F^{\bullet}$ + I^-	-3079.01120695	0.553244	0.450700	0
2-RC	$C_6F^{\bullet}$ + O_2	-1676.88266407	0.075685	0.016752	0
2-PC	$C_6FOO^{\bullet}$	-1676.92775964	0.079285	0.028375	0
3a-RC	$C_6FOO^{\bullet}$ + $C_6FOO^{\bullet}$	-3353.85641238	0.158908	0.071327	0
3a-TS		-3353.83980862	0.159925	0.079667	1
3a-PC	$(C_6FOO)_2$	-3353.87788166	0.160768	0.080275	0
4a-TS		-3353.84092181	0.157603	0.077367	1
4a-PC	$2(C_6FO^{\bullet})$ + O_2	-3353.86377656	0.153437	0.056841	0
3b-RC	$C_6FOO^{\bullet}$ + $C_6F^{\bullet}$	-3203.48238966	0.151013	0.063305	0
3b-TS		-3203.48046153	0.151880	0.074209	1
3b-PC	$(C_6FO)_2$	-3203.59325170	0.155217	0.078390	0
4b-TS		-3203.52190085	0.151025	0.073865	1
4b-PC	$2(C_6FO^{\bullet})$	-3203.53554330	0.149278	0.064130	0
5-RC	$C_6FO^{\bullet}$ + CH_3CN	-1734.53805529	0.120453	0.056841	0
5-TS		-1734.52994168	0.117215	0.060392	1
5-PC	C_6FOH + $\bullet CH_2CN$	-1734.56677616	0.119500	0.049425	0
5b-RC	$C_6FO^{\bullet}$ + H_2O	-1678.20000082	0.097047	0.039924	0
5b-TS		-1678.18740305	0.093522	0.041589	1
5b-PC	C_6FOH + $\bullet OH$	-1678.20559377	0.098083	0.043252	0
6-RC	C_6FOH + CH_3CN	-1735.24090190	0.134460	0.074870	0
6-TS		-1735.20410659	0.131585	0.075278	1
6-PC	C_5FCOF + HF + CH_3CN	-1735.23456506	0.131186	0.066126	0
6b-RC	C_6FOH	-1602.45877022	0.087948	0.039849	0
6b-TS		-1602.38392286	0.081685	0.033039	1
6b-PC	C_5FCOF + HF	-1602.44964681	0.083031	0.027666	0

[a] Computed at 298.15K.

Table S3. Total electronic energies (E), Zero-point energy (ZPE) corrections[a], Thermal corrections to Gibbs free energies[a], and Number of imaginary frequencies of the moieties discussed in Figure S1-S4

Structure	E / Hartree	ZPE corr./ Hartree	Thermal corrections to Gibbs free energies / Hartree	No. of imaginary frequencies
•O=O•	-150.327695551	0.003739	-0.016240	0
•CH_2CN	-132.108644239	0.031197	0.006940	0
CH_3CN	-132.770297271	0.045442	0.021430	0
HF	-100.449765596	0.008831	-0.007615	0

[a] Computed at 298.15K.

Table S4. Cartesian coordinates of the reactant complex for the formation of perfluorohexyl radical ($C_6F^{\bullet}$) by [Ir(ppy)$_3$] (1-RC)

	Coordinates (Angstroms)		
	X	Y	Z
C	4.228577	1.250558	-0.650220
C	4.030986	2.539551	-0.073317
C	4.838251	3.634170	-0.440529
C	5.850953	3.480366	-1.384968
C	6.056290	2.223067	-1.969554
C	5.255942	1.135402	-1.605999
C	2.946854	2.664402	0.915211
N	2.245340	1.519094	1.151521
C	1.230785	1.510923	2.034712
C	0.847904	2.644006	2.741850
C	1.552173	3.832065	2.515655
C	2.600194	3.841638	1.601346
Ir	2.957006	-0.206605	0.000049
N	1.584063	-1.595732	0.909661
C	2.133748	-2.226742	2.050501
C	1.338814	-3.187618	2.756109
C	0.076129	-3.511909	2.323092
C	-0.441231	-2.876331	1.151337
C	0.356570	-1.940663	0.499060
C	3.448928	-1.832018	2.378781
C	4.085855	-0.803354	1.517144
C	5.376743	-0.363407	1.868779
C	6.069915	-0.876947	2.967000
C	5.454829	-1.880074	3.773044
C	4.187345	-2.348328	3.495509
N	1.667127	0.233765	-1.743995
C	1.859250	-0.614338	-2.792188
C	1.127726	-0.434938	-3.979048
C	0.213897	0.608289	-4.082281
C	0.034940	1.470232	-2.995342
C	0.785945	1.244366	-1.847755
C	2.861039	-1.666180	-2.560383
C	3.160922	-2.642321	-3.530224
C	4.115874	-3.624267	-3.277326
C	4.776518	-3.632694	-2.041315
C	4.480126	-2.668224	-1.074558
C	3.523063	-1.657756	-1.297837
H	1.277091	-1.105927	-4.816886
H	-0.666481	2.297015	-3.030784
H	-0.351753	0.748947	-4.998886
H	2.648815	-2.643729	-4.488392
H	5.525044	-4.394149	-1.831603
H	4.342401	-4.373025	-4.031713
H	-0.003505	-1.436018	-0.393210
H	-1.429468	-3.105416	0.767864
H	1.745443	-3.661507	3.643990
H	-0.522336	-4.240692	2.862561
H	5.855965	0.392311	1.252925
H	3.751973	-3.111465	4.134180
H	7.070142	-0.526628	3.207057
H	5.996551	-2.284330	4.625845
H	5.442128	0.171467	-2.072623
H	6.843986	2.092066	-2.709026
H	4.683672	4.612311	0.006783

```
H     6.471613   4.328210  -1.662856
H     0.726081   0.559586   2.165037
H     3.149359   4.758424   1.421183
H     0.024885   2.593246   3.446769
H     1.285771   4.741269   3.047060
H     5.012447  -2.693919  -0.127983
H     0.685928   1.882449  -0.976637
I    -5.435594  -3.610458   0.355972
C    -4.727572  -1.835578  -0.704999
F    -3.467469  -2.046508  -1.147720
C    -4.737085  -0.559177   0.197869
F    -4.082371  -0.833165   1.350248
F    -5.518007  -1.621425  -1.777419
C    -4.053554   0.701924  -0.448981
F    -2.711107   0.524170  -0.401682
F    -6.027479  -0.258150   0.485322
C    -4.411456   2.054953   0.267371
F    -4.431461   0.803957  -1.744837
F    -5.666698   2.409700  -0.098993
F    -4.387028   1.870257   1.609330
C    -3.433953   3.232463  -0.075581
C    -3.961034   4.656136   0.304630
F    -2.272303   3.038680   0.590071
F    -3.181856   3.237165  -1.407399
F    -4.354256   4.690062   1.586968
F    -4.987670   5.013010  -0.477653
F    -2.966927   5.540320   0.134781
---------------------------------------
```

Table S5. Cartesian coordinates of the product complex for the formation of perfluorohexyl radical ($C_6F^{\bullet}$) by [Ir(ppy)$_3$] (1-PC)

	Coordinates (Angstroms)		
	X	Y	Z
C	-3.720158	1.779888	0.995637
C	-3.160290	3.063040	0.736935
C	-3.673906	4.209303	1.370241
C	-4.737952	4.105302	2.263386
C	-5.289503	2.846718	2.536857
C	-4.779168	1.702357	1.918737
C	-2.021967	3.115880	-0.191407
N	-1.634686	1.909732	-0.696866
C	-0.610273	1.837497	-1.567060
C	0.097389	2.959119	-1.979319
C	-0.279752	4.205680	-1.469212
C	-1.340233	4.282637	-0.573374
Ir	-2.877772	0.227240	-0.003115
N	-1.833648	-1.215673	-1.261750
C	-2.366043	-1.330765	-2.513957
C	-1.807418	-2.242985	-3.424116
C	-0.721032	-3.023237	-3.045827
C	-0.191332	-2.890470	-1.756752
C	-0.781990	-1.974545	-0.896807
C	-3.511789	-0.452884	-2.784806
C	-3.928543	0.402742	-1.722170
C	-4.999018	1.281024	-1.972386
C	-5.651357	1.297977	-3.207066
C	-5.236992	0.444115	-4.239486
C	-4.167828	-0.423627	-4.028735
N	-1.718431	-0.150289	1.823293
C	-2.262863	-1.114374	2.617938
C	-1.663592	-1.431207	3.846954
C	-0.521159	-0.750318	4.254681
C	0.016119	0.241335	3.428392
C	-0.617181	0.510141	2.220351
C	-3.475627	-1.741709	2.076722
C	-4.153550	-2.777489	2.736061
C	-5.281718	-3.360024	2.158007
C	-5.735330	-2.918415	0.904655
C	-5.062921	-1.899033	0.235501
C	-3.932931	-1.265794	0.803153
H	-2.089046	-2.201375	4.479174
H	0.905438	0.795909	3.707187
H	-0.054412	-0.989597	5.205344
H	-3.809320	-3.143587	3.698219
H	-6.615174	-3.373190	0.456880
H	-5.802948	-4.158649	2.678024
H	-0.415864	-1.831445	0.113566
H	0.658663	-3.478433	-1.423441
H	-2.222235	-2.339157	-4.420468
H	-0.288455	-3.729470	-3.748325
H	-5.340057	1.949778	-1.188060
H	-3.850033	-1.072890	-4.838955
H	-6.485678	1.976622	-3.367910
H	-5.742507	0.458807	-5.201004
H	-5.229554	0.740305	2.142598
H	-6.121319	2.757905	3.231661
H	-3.247298	5.188175	1.173382

```
H     -5.131996    4.995821    2.744945
H     -0.358191    0.848683   -1.931929
H     -1.640191    5.243390   -0.172356
H      0.918527    2.853240   -2.679824
H      0.247667    5.106899   -1.767334
H     -5.432912   -1.566377   -0.728563
H     -0.241004    1.267972    1.542415
I      3.373397   -4.897816   -0.453085
C      3.704816   -2.146822    0.977424
F      2.494747   -1.864657    1.513373
C      4.180036   -1.047956    0.035622
F      3.319967   -0.993997   -1.020447
F      4.584107   -2.391575    1.972378
C      4.271326    0.404000    0.628528
F      3.005159    0.860139    0.821006
F      5.419611   -1.387617   -0.420796
C      5.051580    1.445560   -0.249670
F      4.889177    0.339779    1.836336
F      6.379518    1.198315   -0.125390
F      4.704005    1.286811   -1.550723
C      4.785800    2.941877    0.135064
C      5.803577    3.969851   -0.461766
F      3.554352    3.291802   -0.305565
F      4.822868    3.077298    1.483825
F      5.918528    3.812069   -1.789376
F      7.011395    3.833912    0.100827
F      5.355493    5.210465   -0.213913
---------------------------------------
```

Table S6. Cartesian coordinates of the reactant complex for the formation of perfluorohexyl peroxyl radical ($C_6FOO^{\bullet}$) by $C_6F^{\bullet}$ and O_2 (2-RC)

	Coordinates (Angstroms)		
	X	Y	Z
C	2.897237	-0.829153	0.158377
F	3.070957	-1.290660	1.389286
F	3.059462	-1.776380	-0.757658
C	1.694782	0.081658	-0.047628
F	1.725093	1.031840	0.923566
F	1.832029	0.674683	-1.261290
C	0.294423	-0.628265	-0.004146
F	0.273445	-1.444261	1.079659
F	0.183664	-1.391394	-1.120122
C	-0.940984	0.337011	0.086320
C	-2.305235	-0.333059	-0.299434
F	-2.381397	-1.559509	0.273355
F	-1.025430	0.797546	1.358323
F	-0.743871	1.390481	-0.742850
C	-3.578550	0.466114	0.135320
F	-4.655729	-0.104505	-0.424204
F	-2.352695	-0.473461	-1.644257
F	-3.502577	1.740855	-0.276851
F	-3.727383	0.444632	1.466127
O	5.349647	0.841426	-0.249345
O	5.379084	2.042993	-0.068232

Table S7. Cartesian coordinates of the product complex for the formation of perfluorohexyl peroxyl radical ($C_6FOO^{\bullet}$) by $C_6F^{\bullet}$ and O_2 (2-PC)

	Coordinates (Angstroms)		
	X	Y	Z
O	5.289023	0.160905	-0.001374
O	4.093545	0.666090	-0.288930
C	3.055844	-0.213372	0.165857
C	1.708797	0.490945	-0.203368
F	3.167013	-0.390758	1.486326
F	3.165919	-1.399301	-0.447799
C	0.438500	-0.409879	-0.002945
F	1.775457	0.861039	-1.502117
F	1.601753	1.598807	0.568238
C	-0.912076	0.393213	0.011119
F	0.404773	-1.315840	-1.008978
F	0.553776	-1.069339	1.174064
F	-1.024285	1.011018	1.211162
F	-0.874678	1.335184	-0.961846
C	-2.182628	-0.496537	-0.220152
C	-3.538664	0.184248	0.164637
F	-2.074564	-1.631344	0.513099
F	-2.248071	-0.825004	-1.530406
F	-3.645381	0.323091	1.492261
F	-4.545027	-0.589620	-0.266910
F	-3.643261	1.391215	-0.412475

Table S8. Cartesian coordinates of the reactant complex for the formation of C_6FOO-OOC_6F by $C_6FOO^{\bullet}$ (3a-RC)

	Coordinates (Angstroms)		
	X	Y	Z
C	0.343481	4.027495	-0.930039
C	-0.214400	3.755746	0.514160
C	0.634695	2.722514	1.336467
C	0.336090	2.724614	2.871715
F	0.780151	3.843034	3.453810
F	0.377670	1.481021	0.866451
F	-0.976289	2.596461	3.109404
F	1.952030	2.994002	1.175571
F	-1.477954	3.277674	0.419364
F	-0.242704	4.930827	1.186399
F	1.419598	4.842602	-0.821024
F	0.740802	2.854127	-1.478552
O	1.036867	1.593358	3.406680
O	0.875707	1.530436	4.724760
O	-0.875707	-1.530436	4.724760
O	-1.036867	-1.593358	3.406680
C	-0.336090	-2.724614	2.871715
C	-0.634695	-2.722514	1.336467
F	-0.780151	-3.843034	3.453810
F	0.976289	-2.596461	3.109404
C	0.214400	-3.755746	0.514160
F	-0.377670	-1.481021	0.866451
F	-1.952030	-2.994002	1.175571
C	-0.343481	-4.027495	-0.930039
F	1.477954	-3.277674	0.419364
F	0.242704	-4.930827	1.186399
F	-1.419598	-4.842602	-0.821024
F	-0.740802	-2.854127	-1.478552
C	0.697170	-4.690095	-1.898096
C	0.082638	-5.314592	-3.195115
C	-0.697170	4.690095	-1.898096
C	-0.082638	5.314592	-3.195115
F	1.353006	-5.678736	-1.242507
F	1.590326	-3.749838	-2.281927
F	-0.634695	-6.408165	-2.907378
F	1.082333	-5.662926	-4.018115
F	-0.703923	-4.426539	-3.822171
F	-1.353006	5.678736	-1.242507
F	-1.590326	3.749838	-2.281927
F	0.703923	4.426539	-3.822171
F	0.634695	6.408165	-2.907378
F	-1.082333	5.662926	-4.018115

Table S9. Cartesian coordinates of the transition state for the formation of C_6FOO-OOC_6F by $C_6FOO^{\bullet}$ (3a-TS)

	Coordinates (Angstroms)		
	X	Y	Z
C	-5.641225	0.764970	0.037927
C	-4.894632	-0.582632	-0.273863
C	-3.353018	-0.409075	-0.517068
C	-2.538581	-1.742769	-0.425328
F	-2.459901	-2.175544	0.839826
F	-3.167730	0.110000	-1.752045
F	-3.098742	-2.703160	-1.177057
F	-2.845604	0.445586	0.402943
F	-5.433266	-1.142010	-1.383229
F	-5.080253	-1.422997	0.771736
F	-5.372422	1.109647	1.319802
F	-5.165668	1.733080	-0.782092
O	-1.237728	-1.433474	-0.911192
O	-0.456668	-2.523311	-0.879955
O	0.494192	-2.553084	0.935941
O	1.807832	-2.504642	0.667266
C	2.266510	-1.157301	0.657680
C	3.801957	-1.236712	0.363996
F	2.027399	-0.587395	1.846494
F	1.632000	-0.455352	-0.292761
C	4.480080	0.155509	0.104678
F	3.975013	-2.010543	-0.731356
F	4.394456	-1.832727	1.426322
C	6.050429	0.117805	0.176348
F	4.102034	0.583390	-1.123361
F	4.034637	1.038594	1.029374
F	6.412694	0.071416	1.480583
F	6.495303	-1.004486	-0.438380
C	6.745746	1.350791	-0.498111
C	8.258186	1.532465	-0.138419
C	-7.196039	0.687995	-0.149664
C	-7.995357	1.871553	0.490706
F	6.101041	2.484515	-0.128717
F	6.661237	1.214724	-1.841163
F	8.407236	1.892819	1.142674
F	8.770066	2.497279	-0.916491
F	8.937283	0.396039	-0.356511
F	-7.656820	-0.460610	0.403320
F	-7.472710	0.680240	-1.473612
F	-7.500788	3.051112	0.085341
F	-7.950384	1.814199	1.827819
F	-9.275597	1.783353	0.101679

Table S10. Cartesian coordinates of the product complex for the formation of C_6FOO-OOC_6F by $C_6FOO^{\bullet}$ (3a-PC)

	Coordinates (Angstroms)		
	X	Y	Z
C	-4.806246	-0.534738	-0.308432
C	-3.596524	0.178749	0.398405
C	-2.988232	1.362451	-0.436883
C	-2.074391	2.333051	0.400398
F	-2.832688	3.065338	1.249030
F	-2.249472	0.838810	-1.440845
F	-1.205479	1.617561	1.153706
F	-3.995275	2.097021	-0.966328
F	-2.616857	-0.730518	0.616746
F	-4.025137	0.653399	1.591553
F	-5.899304	0.254453	-0.177198
F	-4.528209	-0.677019	-1.626862
O	-1.436988	3.129209	-0.519405
O	-0.605426	4.143072	0.252909
O	0.605499	4.143121	-0.253027
O	1.437224	3.129420	0.519342
C	2.074490	2.333086	-0.400413
C	2.988477	1.362647	0.436874
F	2.832649	3.065222	-1.249308
F	1.205448	1.617466	-1.153441
C	3.596415	0.178657	-0.398283
F	2.249970	0.839317	1.441183
F	3.995723	2.097281	0.965848
C	4.806394	-0.534647	0.308289
F	2.616627	-0.730647	-0.615917
F	4.024556	0.652899	-1.591761
F	5.899461	0.254393	0.176221
F	4.528943	-0.676362	1.626900
C	-5.135224	-1.953224	0.274076
C	-6.538182	-2.519040	-0.128598
C	5.134971	-1.953417	-0.273782
C	6.538073	-2.519183	0.128438
F	5.089766	-1.905015	-1.627734
F	4.201714	-2.828220	0.165627
F	7.520879	-1.836617	-0.472899
F	6.609947	-3.801537	-0.257084
F	6.711236	-2.457636	1.457680
F	-4.201828	-2.828302	-0.164489
F	-5.090692	-1.904229	1.628029
F	-6.710665	-2.458110	-1.457958
F	-7.521219	-1.836073	0.471905
F	-6.610384	-3.801203	0.257497

Table S11. Cartesian coordinates of the transition state for the formation of $C_6FO^{\bullet}$ and O_2 by $C_6FOO\text{-}OOC_6F$ (4a-TS)

	Coordinates (Angstroms)		
	X	Y	Z
C	-0.511203	-6.007000	-0.795535
C	-0.762259	-5.176352	0.518379
C	0.043050	-3.822753	0.561918
C	-0.502031	-2.776952	1.644660
F	-1.724281	-2.326558	1.214784
F	1.330127	-4.112470	0.845157
F	-0.745349	-3.460182	2.813261
F	-0.019700	-3.229437	-0.650859
F	-0.390403	-5.923953	1.584047
F	-2.087172	-4.922335	0.603455
F	-1.216003	-5.434134	-1.800275
F	0.806162	-5.961761	-1.107779
O	0.396438	-1.828972	1.762987
O	0.344946	0.472511	3.147180
O	-0.344946	-0.472511	3.147180
O	-0.396438	1.828972	1.762987
C	0.502031	2.776952	1.644660
C	-0.043050	3.822753	0.561918
F	1.724281	2.326558	1.214784
F	0.745349	3.460182	2.813261
C	0.762259	5.176352	0.518379
F	-1.330127	4.112470	0.845157
F	0.019700	3.229437	-0.650859
C	0.511203	6.007000	-0.795535
F	0.390403	5.923953	1.584047
F	2.087172	4.922335	0.603455
F	1.216003	5.434134	-1.800275
F	-0.806162	5.961761	-1.107779
C	-0.929401	-7.514961	-0.681407
C	-1.048954	-8.268548	-2.048279
C	0.929401	7.514961	-0.681407
C	1.048954	8.268548	-2.048279
F	2.131949	7.603856	-0.062743
F	0.004663	8.165419	0.061191
F	2.101397	7.827854	-2.749334
F	1.216003	9.576456	-1.803320
F	-0.064724	8.105064	-2.778667
F	-0.004663	-8.165419	0.061191
F	-2.131949	-7.603856	-0.062743
F	0.064724	-8.105064	-2.778667
F	-2.101397	-7.827854	-2.749334
F	-1.216003	-9.576456	-1.803320

Table S12. Cartesian coordinates of the product complex for the formation of $C_6FO^{\bullet}$ and O_2 by $C_6FOO\text{-}OOC_6F$ (4a-PC)

	Coordinates (Angstroms)		
	X	Y	Z
C	0.348498	5.474933	-0.615295
C	-0.184391	4.179538	0.104906
C	0.871880	3.545871	1.090796
C	0.206119	2.520607	2.141099
F	-0.512373	3.236947	3.048278
F	1.796162	2.892945	0.361093
F	-0.681240	1.724205	1.478276
F	1.468960	4.523601	1.800113
F	-0.494553	3.253997	-0.830524
F	-1.302132	4.506952	0.788868
F	0.301464	6.499706	0.267820
F	1.635941	5.278297	-0.986640
O	1.210899	1.855379	2.684938
O	-0.575280	0.195526	5.585706
O	0.575280	-0.195526	5.585706
O	-1.210899	-1.855379	2.684938
C	-0.206119	-2.520607	2.141099
C	-0.871880	-3.545871	1.090796
F	0.512373	-3.236947	3.048278
F	0.681240	-1.724205	1.478276
C	0.184391	-4.179538	0.104906
F	-1.796162	-2.892945	0.361093
F	-1.468960	-4.523601	1.800113
C	-0.348498	-5.474933	-0.615295
F	0.494553	-3.253997	-0.830524
F	1.302132	-4.506952	0.788868
F	-0.301464	-6.499706	0.267820
F	-1.635941	-5.278297	-0.986640
C	-0.471982	5.868596	-1.893652
C	-0.228113	7.328513	-2.403626
C	0.471982	-5.868596	-1.893652
C	0.228113	-7.328513	-2.403626
F	1.796162	-5.744103	-1.634365
F	0.139609	-5.025111	-2.896884
F	0.748804	-8.225523	-1.556692
F	0.823115	-7.470471	-3.596726
F	-1.084656	-7.567791	-2.543785
F	-0.139609	5.025111	-2.896884
F	-1.796162	5.744103	-1.634365
F	1.084656	7.567791	-2.543785
F	-0.748804	8.225523	-1.556692
F	-0.823115	7.470471	-3.596726

Table S13. Cartesian coordinates of the reactant complex for the formation of C_6FOOC_6F by $C_6FOO^{\bullet}$ and $C_6F^{\bullet}$ (3b-RC)

	Coordinates (Angstroms)		
	X	Y	Z
C	6.187779	-0.018522	0.214935
C	4.712738	-0.174500	-0.304854
C	3.849503	1.128519	-0.155374
C	2.308908	0.896145	-0.294519
F	2.020090	0.223176	-1.416677
F	4.071623	1.677607	1.062836
F	1.819285	0.229000	0.755135
F	4.224476	2.007415	-1.112128
F	4.119462	-1.172782	0.391462
F	4.737320	-0.512885	-1.615840
F	6.667990	1.186016	-0.177585
F	6.165024	-0.058022	1.568520
O	1.721339	2.203526	-0.350275
O	0.397220	2.112998	-0.428495
C	-3.147678	2.321450	0.336753
C	-3.784933	1.037754	-0.176940
F	-3.694440	3.446631	-0.108618
F	-2.902108	2.367397	1.639253
C	-5.290371	0.827457	0.218631
F	-3.062936	-0.006281	0.308126
F	-3.699780	1.051853	-1.532088
C	-5.859302	-0.610308	-0.054922
F	-5.413397	1.085073	1.545209
F	-6.028066	1.736220	-0.467229
F	-5.420632	-1.039586	-1.262912
F	-5.379692	-1.443584	0.900438
C	7.167034	-1.126671	-0.306166
F	6.562945	-2.336729	-0.215677
F	7.454349	-0.875086	-1.603578
C	8.524562	-1.219754	0.467835
F	8.338980	-1.692752	1.706825
F	9.337743	-2.056851	-0.192398
F	9.111527	-0.015417	0.541394
C	-7.425474	-0.689228	-0.052883
C	-8.013931	-2.135799	0.047837
F	-7.887852	-0.141997	-1.200739
F	-7.909458	0.018645	0.997278
F	-9.338970	-2.074389	-0.151339
F	-7.473879	-2.934102	-0.885759
F	-7.788659	-2.663175	1.258107

Table S14. Cartesian coordinates of the transition state for the formation of C_6FOOC_6F by $C_6FOO^{\bullet}$ and $C_6F^{\bullet}$ (3b-TS)

	Coordinates (Angstroms)		
	X	Y	Z
C	5.090344	0.252351	-0.351727
C	3.935529	-0.175952	0.624996
C	2.945580	-1.229843	0.012750
C	1.581369	-1.364643	0.771262
F	1.810314	-1.452529	2.110439
F	2.675519	-0.884772	-1.272784
F	0.841515	-0.243940	0.572718
F	3.563173	-2.435452	0.017108
F	3.245918	0.937463	0.970726
F	4.485497	-0.710276	1.742855
F	5.548843	-0.842119	-1.006420
F	4.579570	1.119207	-1.259663
O	0.966270	-2.484224	0.280732
O	-0.283988	-2.666012	0.911252
C	-1.963842	-1.835249	-0.926831
C	-2.872805	-1.104555	0.073260
F	-2.358207	-2.950795	-1.421960
F	-1.146008	-1.168409	-1.651681
C	-4.165750	-0.532329	-0.629796
F	-2.176203	-0.086332	0.607346
F	-3.239134	-1.982914	1.022293
C	-4.975105	0.492183	0.244465
F	-3.767528	0.084647	-1.768394
F	-4.953787	-1.582249	-0.952833
F	-5.028540	0.034227	1.516935
F	-4.310384	1.670599	0.231445
C	6.309423	0.933163	0.362153
F	5.855564	1.821264	1.280268
F	7.030013	-0.021598	0.994110
C	7.283360	1.702968	-0.591376
F	6.707952	2.813196	-1.071069
F	8.375748	2.054038	0.103061
F	7.657006	0.924279	-1.618496
C	-6.442637	0.727208	-0.257075
C	-7.147602	1.989142	0.343377
F	-7.187125	-0.352793	0.069995
F	-6.434842	0.865560	-1.605187
F	-8.441045	1.964544	-0.007757
F	-7.062100	1.985630	1.682126
F	-6.596778	3.114548	-0.128362

Table S15. Cartesian coordinates of the product complex for the formation of C_6FOOC_6F by $C_6FOO^{\bullet}$ and $C_6F^{\bullet}$ (3b-PC)

	Coordinates (Angstroms)		
	X	Y	Z
C	-5.530184	-0.255794	-0.104712
C	-4.105508	0.313621	0.240210
C	-2.936475	-0.692079	-0.062021
C	-1.579653	-0.317514	0.640055
F	-1.293734	0.987545	0.448306
F	-3.291557	-1.929129	0.357929
F	-1.666296	-0.526464	1.968601
F	-2.732754	-0.720931	-1.398150
F	-4.084434	0.632851	1.555558
F	-3.891849	1.437092	-0.484870
F	-5.465778	-0.928283	-1.279120
F	-5.888415	-1.121540	0.873472
O	-0.635714	-1.147973	0.061641
O	0.630399	-0.895898	0.739001
C	1.573949	-0.653180	-0.244402
C	2.914018	-0.375593	0.531469
F	1.247092	0.408157	-1.005203
F	1.714641	-1.718043	-1.064378
C	4.188365	-0.376685	-0.388164
F	3.069649	-1.328168	1.477649
F	2.798785	0.831247	1.134418
C	5.444764	0.295592	0.275736
F	4.485764	-1.662094	-0.693000
F	3.907482	0.289761	-1.532426
F	5.281895	1.639288	0.226027
F	5.516853	-0.086240	1.573626
C	-6.639186	0.845326	-0.235770
F	-6.510765	1.734679	0.779101
F	-6.469710	1.492607	-1.411204
C	-8.107864	0.305445	-0.203091
F	-8.424999	-0.149306	1.015875
F	-8.940265	1.309398	-0.515042
F	-8.269237	-0.682969	-1.096007
C	6.802449	-0.075257	-0.416487
C	8.005454	0.853385	-0.041592
F	6.650422	-0.018978	-1.762215
F	7.136587	-1.337721	-0.064536
F	9.132020	0.313798	-0.529063
F	7.852243	2.073508	-0.571767
F	8.121001	0.965199	1.290582

Table S16. Cartesian coordinates of the transition state for the formation of $C_6FO^{\bullet}$ by C_6FOOC_6F (4b-TS)

	Coordinates (Angstroms)		
	X	Y	Z
C	4.855033	-0.476543	-0.368513
C	4.064045	0.655391	0.381780
C	2.735930	1.087464	-0.334090
C	2.133681	2.460718	0.133680
F	2.083967	2.484887	1.490689
F	2.965036	1.187310	-1.669171
F	2.979052	3.456476	-0.281664
F	1.816613	0.116354	-0.127267
F	4.881725	1.729686	0.496624
F	3.749131	0.216791	1.625770
F	3.979467	-1.405965	-0.822788
F	5.487323	0.079376	-1.430586
O	0.959287	2.790475	-0.442625
O	-0.503489	1.506010	0.582281
C	-1.442852	1.457426	-0.293130
C	-2.582984	0.488782	0.541040
F	-1.171046	0.814085	-1.446551
F	-2.061103	2.617359	-0.603725
C	-3.976057	0.523214	-0.224222
F	-2.756549	0.957266	1.772148
F	-2.096098	-0.749289	0.569033
C	-4.925675	-0.650472	0.249046
F	-4.564816	1.704961	0.038933
F	-3.783072	0.400778	-1.548444
F	-4.486608	-1.795434	-0.318221
F	-4.849211	-0.769570	1.593499
C	5.917982	-1.209651	0.521439
F	6.606650	-0.294886	1.247166
F	5.272861	-2.045150	1.367782
C	6.964726	-2.060958	-0.271785
F	7.800426	-1.274048	-0.961803
F	7.681645	-2.782637	0.602369
F	6.350038	-2.898600	-1.120964
C	-6.431223	-0.425089	-0.140243
C	-7.332867	-1.700560	-0.022898
F	-6.503183	0.010511	-1.420123
F	-6.948758	0.518390	0.676805
F	-8.610569	-1.335866	-0.197089
F	-7.011620	-2.600776	-0.959973
F	-7.202949	-2.260921	1.188677

Table S17. Cartesian coordinates of the product complex for the formation of $C_6FO^{\bullet}$ by C_6FOOC_6F (4b-PC)

	Coordinates (Angstroms)		
	X	Y	Z
C	-6.612577	0.373628	-0.127245
C	-5.206306	-0.276828	0.155449
C	-4.004003	0.693440	-0.165168
C	-2.601163	-0.084937	-0.318541
F	-2.494037	-1.002180	0.685717
F	-4.241203	1.336098	-1.325381
F	-2.620922	-0.782995	-1.486748
F	-3.904806	1.591570	0.833169
F	-5.099687	-1.392868	-0.597757
F	-5.134483	-0.616929	1.462038
F	-6.603712	1.655983	0.307722
F	-6.819176	0.369109	-1.465097
O	-1.662208	0.845385	-0.287208
O	1.727993	-0.752507	-0.895676
C	2.585868	-0.096174	-0.133317
C	4.050164	-0.605917	-0.572088
F	2.420539	-0.349537	1.193676
F	2.526632	1.258248	-0.285287
C	5.206547	0.309569	-0.010669
F	4.131038	-0.615926	-1.916141
F	4.200600	-1.860521	-0.104217
C	6.615822	-0.393111	-0.041165
F	5.257964	1.430174	-0.765241
F	4.934261	0.650711	1.267585
F	6.670232	-1.275194	0.984395
F	6.748886	-1.070862	-1.206236
C	-7.803679	-0.370726	0.573264
F	-7.647670	-1.708544	0.424044
F	-7.784808	-0.070616	1.891526
C	-9.222378	-0.000037	0.024469
F	-9.396588	-0.478105	-1.214166
F	-10.147645	-0.544788	0.827370
F	-9.392432	1.330712	0.009514
C	7.821407	0.603762	0.083152
C	9.189533	-0.066226	0.444726
F	7.550969	1.519251	1.044866
F	7.978442	1.241779	-1.098588
F	10.161817	0.848296	0.316843
F	9.185297	-0.511808	1.707460
F	9.449194	-1.091245	-0.381523

Table S18. Cartesian coordinates of the reactant complex for the formation of C_6FOH by $C_6FO^{\bullet}$ and CH_3CN (5-RC)

	Coordinates (Angstroms)		
	X	Y	Z
O	3.328891	0.392585	0.536286
C	2.280343	0.862127	-0.118044
C	1.017390	0.000361	0.392574
F	2.384672	0.718281	-1.467235
F	2.036411	2.182937	0.119195
C	-0.363730	0.638359	-0.026222
F	1.056265	-0.085444	1.735691
F	1.124006	-1.232683	-0.139714
C	-1.564036	-0.377317	0.069991
F	-0.608112	1.685515	0.793202
F	-0.288978	1.082257	-1.299638
F	-1.502109	-1.207161	-0.997585
F	-1.435257	-1.111677	1.200453
C	-2.973031	0.313107	0.095813
C	-4.177678	-0.644262	-0.192513
F	-3.007299	1.300247	-0.831906
F	-3.166314	0.853832	1.320017
F	-4.178646	-1.042609	-1.470885
F	-5.317942	0.018037	0.050312
F	-4.126476	-1.723041	0.603656
H	6.770615	-2.505875	0.757894
H	5.550355	-1.489988	-0.049211
C	6.579411	-1.857719	-0.102579
H	6.702109	-2.440483	-1.020414
C	7.510682	-0.732966	-0.097143
N	8.251099	0.162731	-0.092840

Table S19. Cartesian coordinates of the transition state for the formation of C_6FOH by $C_6FO^{\bullet}$ and CH_3CN (5-TS)

	Coordinates (Angstroms)		
	X	Y	Z
O	3.618485	0.780326	0.499816
C	2.463068	1.074537	-0.129882
C	1.233853	0.242680	0.382392
F	2.563055	0.907140	-1.481370
F	2.222096	2.395080	0.116236
C	-0.176465	0.728455	-0.101347
F	1.249552	0.279774	1.735804
F	1.417042	-1.046601	-0.016617
C	-1.323305	-0.326086	0.107267
F	-0.490850	1.856222	0.583493
F	-0.119752	1.025810	-1.421451
F	-1.211115	-1.271335	-0.857723
F	-1.169026	-0.920236	1.315517
C	-2.767818	0.282006	0.049232
C	-3.915948	-0.766883	-0.127857
F	-2.850036	1.151106	-0.988014
F	-3.003608	0.950781	1.201407
F	-3.890039	-1.305565	-1.353770
F	-5.093192	-0.146976	0.041374
F	-3.809236	-1.746312	0.783271
H	4.140350	-2.272487	0.609936
H	4.113347	-0.525108	0.139058
C	4.553091	-1.600492	-0.146510
H	4.180720	-1.803367	-1.153373
C	5.981968	-1.488371	-0.084925
N	7.141859	-1.382388	-0.029683

Table S20. Cartesian coordinates of the product complex for the formation of C_6FOH by $C_6FO^{\bullet}$ and CH_3CN (5-PC)

	Coordinates (Angstroms)		
	X	Y	Z
O	-3.330829	1.073883	-0.245169
C	-2.103910	1.393847	0.219152
C	-0.995363	0.381663	-0.239916
F	-2.173487	1.391187	1.567633
F	-1.718381	2.648030	-0.179399
C	0.484818	0.802798	0.054691
F	-1.131382	0.217233	-1.583709
F	-1.246696	-0.806877	0.364368
C	1.516768	-0.378806	-0.036955
F	0.841113	1.761188	-0.835481
F	0.553177	1.323266	1.304040
F	1.397048	-1.136777	1.080070
F	1.218124	-1.144004	-1.115385
C	3.009004	0.083930	-0.171420
C	4.071536	-1.031631	0.105578
F	3.246983	1.094770	0.700151
F	3.212414	0.533878	-1.431035
F	4.092730	-1.363573	1.402898
F	5.281900	-0.565116	-0.235586
F	3.810781	-2.128048	-0.622868
H	-6.601363	-3.211327	-0.225852
C	-6.953510	-2.410857	0.415299
H	-6.601866	-2.342632	1.438778
C	-7.852010	-1.476429	-0.072798
N	-8.615511	-0.682551	-0.488014
H	-3.364480	1.127233	-1.218527

Table S21. Cartesian coordinates of the reactant complex for the formation of C_6FOH by $C_6FO^{\bullet}$ and H_2O (5b-RC)

	Coordinates (Angstroms)		
	X	Y	Z
O	3.978114	-0.249381	-0.493185
C	2.941370	-0.753773	0.152635
C	1.652411	0.069135	-0.376895
F	3.020858	-0.603879	1.500861
F	2.742999	-2.078698	-0.090587
C	0.290455	-0.618954	0.030337
F	1.702466	0.152928	-1.718182
F	1.712368	1.303750	0.155262
C	-0.941908	0.357424	-0.074076
F	0.089566	-1.670619	-0.794385
F	0.369425	-1.063396	1.302636
F	-0.914556	1.186924	0.994845
F	-0.828279	1.096770	-1.202652
C	-2.327111	-0.379516	-0.111620
C	-3.564510	0.536404	0.173643
F	-2.334000	-1.371559	0.811274
F	-2.494144	-0.920447	-1.339473
F	-3.587805	0.925314	1.454627
F	-4.680753	-0.160610	-0.082644
F	-3.541976	1.621909	-0.614654
O	5.862972	2.153734	0.282330
H	6.405867	2.299873	-0.508744
H	5.255668	1.435504	0.039083

Table S22. Cartesian coordinates of the transition state for the formation of C_6FOH by $C_6FO^{\bullet}$ and H_2O (5b-TS)

	Coordinates (Angstroms)		
	X	Y	Z
O	-4.125919	-0.034535	-0.503263
C	-3.036512	-0.660850	-0.087076
C	-1.718426	0.163887	-0.348450
F	-2.930344	-1.851668	-0.752109
F	-3.068954	-0.964983	1.259496
C	-0.404015	-0.422288	0.278656
F	-1.896612	1.411439	0.160945
F	-1.559079	0.268656	-1.691108
C	0.913672	0.180120	-0.332465
F	-0.417803	-0.170760	1.610911
F	-0.373988	-1.762799	0.091026
F	1.116402	-0.384572	-1.547656
F	0.758908	1.516785	-0.495556
C	2.190665	-0.052901	0.547816
C	3.549814	0.181706	-0.192347
F	2.195668	-1.328009	1.007915
F	2.151064	0.793606	1.602543
F	3.772432	-0.775440	-1.102321
F	4.541367	0.151281	0.710380
F	3.558459	1.376930	-0.802412
O	-4.724233	2.029826	0.379458
H	-4.219867	2.247102	1.195422
H	-4.577782	0.928337	0.129722

Table S23. Cartesian coordinates of the product complex for the formation of C_6FOH by $C_6FO^{\bullet}$ and H_2O (5b-PC)

	Coordinates (Angstroms)		
	X	Y	Z
O	4.119335	-0.214384	0.546324
C	3.012844	-0.727204	-0.006730
C	1.702545	0.020900	0.429719
F	2.917846	-2.024648	0.373856
F	3.061615	-0.704245	-1.382862
C	0.394012	-0.365755	-0.340165
F	1.917879	1.353189	0.253928
F	1.517932	-0.209766	1.755201
C	-0.929583	0.087005	0.375941
F	0.436846	0.203461	-1.570535
F	0.349288	-1.712308	-0.487094
F	-1.164844	-0.756085	1.410794
F	-0.763065	1.339945	0.866385
C	-2.189880	0.098712	-0.557243
C	-3.562425	0.172197	0.191034
F	-2.201545	-1.026290	-1.313735
F	-2.115815	1.175374	-1.373558
F	-3.815087	-0.968311	0.846033
F	-4.533883	0.369325	-0.712753
F	-3.573042	1.190914	1.064539
O	4.881455	2.333558	-0.195338
H	4.804008	2.554211	-1.153067
H	4.317454	0.702256	0.218035

Table S24. Cartesian coordinates of the reactant complex for the formation of C_6FCOF by C_6FOH in the presence of CH_3CN (6-RC)

	Coordinates (Angstroms)		
	X	Y	Z
O	3.267853	0.929341	-0.390770
C	2.343109	0.036141	-0.061165
C	0.926784	0.674649	-0.243497
F	2.466905	-0.396099	1.238809
F	2.407326	-1.109717	-0.829034
C	-0.283136	-0.320806	-0.158991
F	0.882209	1.277033	-1.457672
F	0.775037	1.628809	0.713826
C	-1.667941	0.380977	0.086993
F	-0.349557	-1.012060	-1.324593
F	-0.078207	-1.198990	0.852215
F	-1.741714	0.732880	1.394276
F	-1.740941	1.504184	-0.668446
C	-2.908723	-0.513098	-0.261092
C	-4.266658	-0.009804	0.332534
F	-2.706183	-1.770550	0.203504
F	-3.046266	-0.560437	-1.606347
F	-4.295212	-0.161479	1.662993
F	-5.263302	-0.732402	-0.200584
F	-4.464679	1.283710	0.034778
H	4.195281	0.594985	-0.207529
N	5.859050	0.148861	0.055464
C	6.969589	-0.150183	0.196051
C	8.366444	-0.526146	0.371570
H	8.493603	-1.043434	1.327119
H	8.674138	-1.191634	-0.440345
H	8.995259	0.369023	0.360708

Table S25. Cartesian coordinates of the transition state for the formation of C_6FCOF by C_6FOH in the presence of CH_3CN (6-TS)

	Coordinates (Angstroms)		
	X	Y	Z
O	-3.317690	1.448774	0.487333
C	-2.359318	1.127656	-0.225435
C	-0.983686	0.851541	0.480157
F	-2.064818	1.986363	-1.319803
F	-2.637959	-0.174693	-0.962308
C	0.147079	0.114812	-0.316151
F	-1.225569	0.110279	1.598322
F	-0.487912	2.061400	0.889804
C	1.585071	0.277517	0.299418
F	-0.141470	-1.213340	-0.355766
F	0.203098	0.578684	-1.588685
F	2.050455	1.514060	-0.011485
F	1.517788	0.170267	1.650046
C	2.625306	-0.782256	-0.206492
C	4.122744	-0.417735	0.065675
F	2.492578	-0.951573	-1.545499
F	2.379942	-1.962958	0.409249
F	4.516593	0.607086	-0.702081
F	4.884927	-1.483680	-0.224864
F	4.309425	-0.095198	1.355098
H	-4.271059	-0.253310	-0.228846
N	-5.193955	-0.701163	-0.075582
C	-6.217355	-1.187081	0.095855
C	-7.507038	-1.800197	0.312460
H	-8.275248	-1.201722	-0.187391
H	-7.496803	-2.813141	-0.102111
H	-7.708210	-1.839694	1.387577

Table S26. Cartesian coordinates of the product complex for the formation of C_6FCOF by C_6FOH in the presence of CH_3CN (6-PC)

	Coordinates (Angstroms)		
	X	Y	Z
O	-2.636456	-3.084176	-0.816751
C	-2.077828	-2.588841	0.102422
C	-0.544546	-2.353328	0.202201
F	-2.694148	-2.190814	1.223445
F	-3.678074	-0.068845	-0.982014
C	-0.131661	-0.875182	-0.107642
F	0.052646	-3.174947	-0.687369
F	-0.127908	-2.677920	1.453257
C	1.366458	-0.529852	0.213200
F	-0.371691	-0.652189	-1.422777
F	-0.920313	-0.054787	0.626871
F	1.489428	-0.395241	1.555999
F	2.157651	-1.551007	-0.193702
C	1.877049	0.783324	-0.475665
C	3.205261	1.362440	0.116157
F	0.930159	1.746881	-0.364780
F	2.091120	0.527684	-1.786551
F	3.005040	1.861767	1.342638
F	3.636154	2.349797	-0.682489
F	4.151497	0.413174	0.178457
H	-3.713421	0.859595	-0.693802
N	-3.788231	2.438412	-0.211087
C	-3.843456	3.544556	0.126932
C	-3.913920	4.936083	0.551921
H	-2.936545	5.259705	0.921821
H	-4.205313	5.566479	-0.293346
H	-4.653652	5.041583	1.350926

Table S27. Cartesian coordinates of the reactant complex for the formation of C_6FCOF by C_6FOH (6b-RC)

	Coordinates (Angstroms)		
	X	Y	Z
O	4.300960	0.641026	-0.291935
C	3.312285	-0.150734	0.152204
C	1.946135	0.519986	-0.211284
F	3.374214	-0.341521	1.504751
F	3.357926	-1.403909	-0.403684
C	0.684193	-0.392852	-0.018737
F	1.991530	0.902946	-1.509767
F	1.809769	1.628389	0.561941
C	-0.673883	0.397439	0.015018
F	0.643552	-1.282744	-1.041111
F	0.798154	-1.075484	1.145719
F	-0.791448	0.990595	1.227994
F	-0.653582	1.360276	-0.938515
C	-1.938264	-0.497721	-0.229977
C	-3.298481	0.162147	0.175415
F	-1.820267	-1.648585	0.476691
F	-2.008884	-0.797584	-1.547324
F	-3.401839	0.270604	1.506335
F	-4.300365	-0.611022	-0.268931
F	-3.417617	1.380710	-0.374129
H	5.170132	0.288158	-0.020079

Table S28. Cartesian coordinates of the transition state for the formation of C_6FCOF by C_6FOH (6b-TS)

	Coordinates (Angstroms)		
	X	Y	Z
O	-4.391016	-0.320221	-0.348026
C	-3.314330	-0.144066	0.284505
C	-1.929838	-0.560184	-0.298796
F	-3.319967	-0.148555	1.598327
F	-3.398108	1.607540	-0.219244
C	-0.694756	0.336480	0.078068
F	-2.038858	-0.606844	-1.638574
F	-1.722414	-1.823719	0.170174
C	0.682249	-0.409693	-0.061876
F	-0.685478	1.416306	-0.734933
F	-0.821888	0.753314	1.359544
F	0.828382	-1.240440	0.997946
F	0.667758	-1.149233	-1.197789
C	1.921359	0.550092	-0.123995
C	3.301344	-0.144571	0.126069
F	1.782561	1.524789	0.807728
F	1.968888	1.118470	-1.350391
F	3.421834	-0.527671	1.403614
F	4.278843	0.730394	-0.151770
F	3.442239	-1.216751	-0.668529
H	-4.302173	0.855019	-0.624587

Table S29. Cartesian coordinates of the product complex for the formation of C_6FCOF by C_6FOH (6b-PC)

	Coordinates (Angstroms)		
	X	Y	Z
O	-3.988317	-0.173392	-0.935938
C	-3.289773	-0.409696	-0.009075
C	-1.871651	-1.040341	-0.090650
F	-3.636586	-0.174754	1.263723
F	-3.402928	2.960568	0.082736
C	-0.742866	0.045418	-0.091048
F	-1.804108	-1.751560	-1.236486
F	-1.687628	-1.876190	0.961453
C	0.711213	-0.516927	0.093256
F	-0.822548	0.717215	-1.265289
F	-0.997415	0.910392	0.921745
F	0.874666	-0.839567	1.398842
F	0.850202	-1.639468	-0.651619
C	1.839546	0.488476	-0.324896
C	3.271892	0.121023	0.187951
F	1.540264	1.721178	0.153392
F	1.891221	0.542534	-1.675312
F	3.359548	0.274524	1.515416
F	4.159552	0.938339	-0.396965
F	3.578045	-1.146477	-0.128329
H	-2.724209	3.528794	0.404507

5. ^{1}H, ^{19}F and $^{13}C\{^{1}H\}$ NMR Spectra of the Ester Products

^{1}H NMR Spectrum

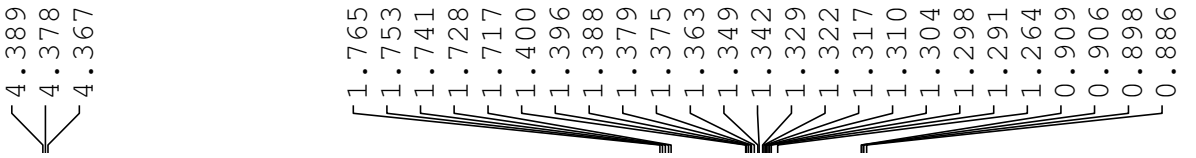

2a

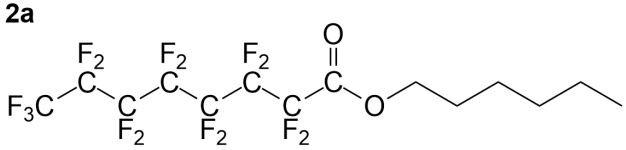

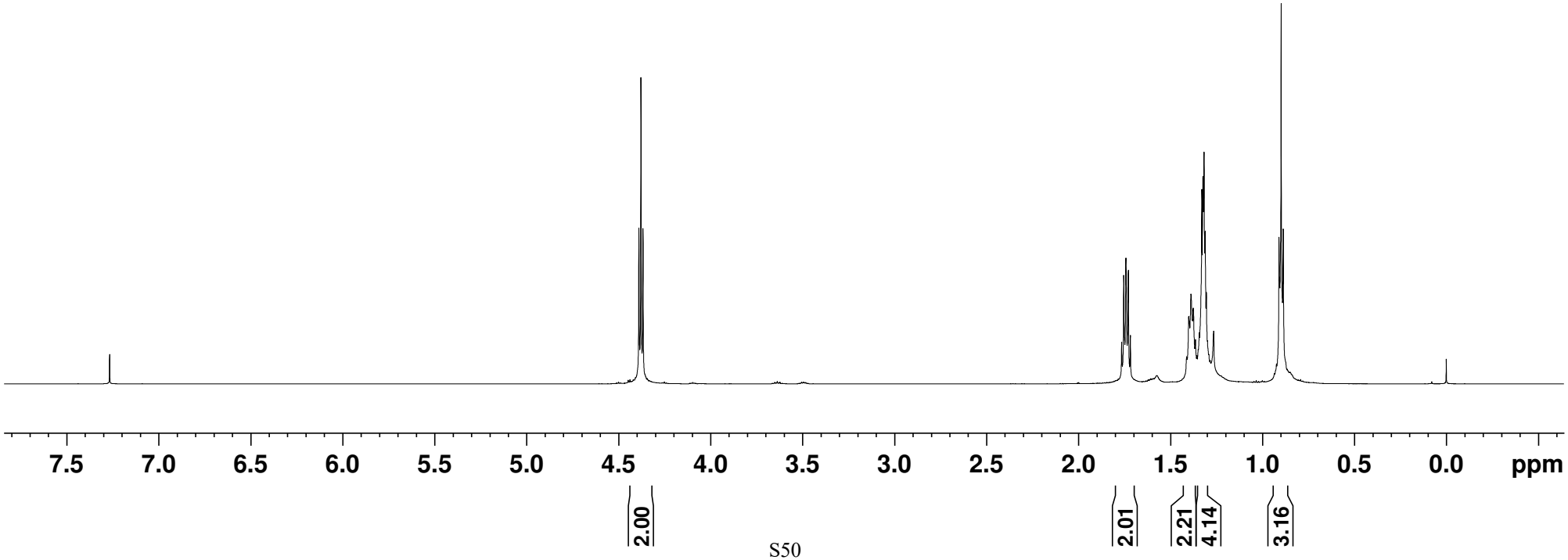

^{19}F NMR Spectrum

2a

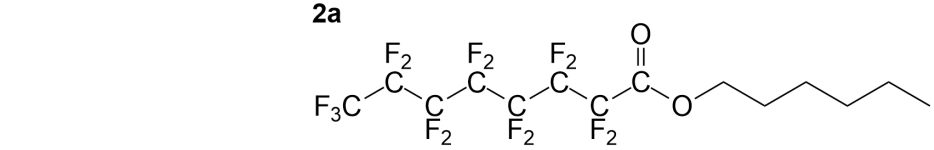

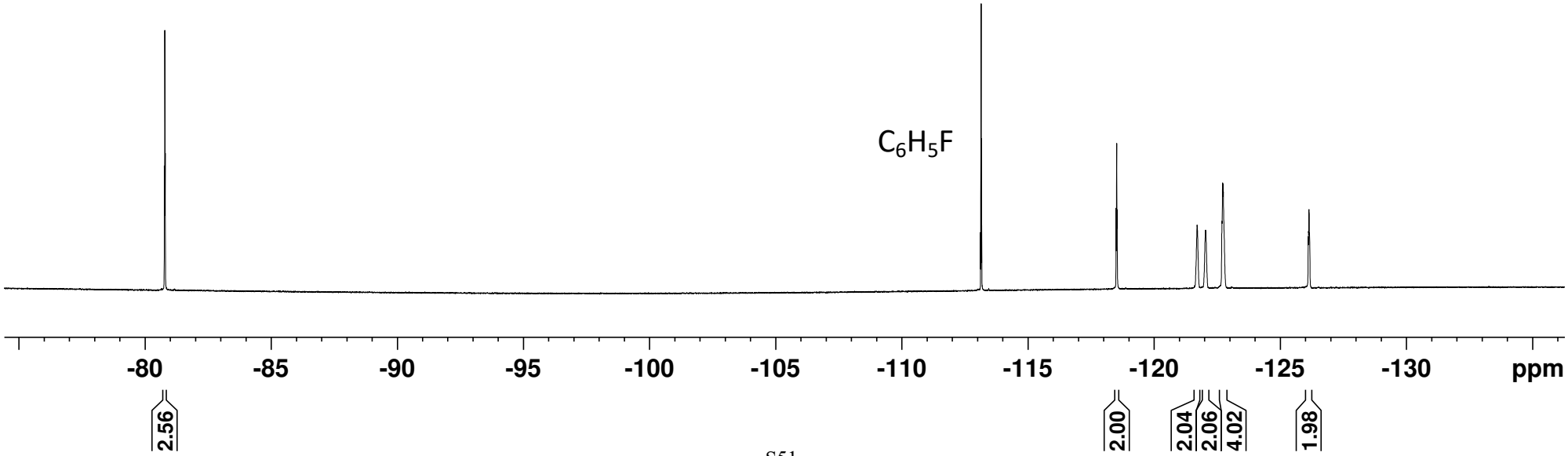

$^{13}C\{^{1}H\}$ NMR Spectrum

158.75
158.56
158.36
68.83
31.30
28.21
25.26
22.53
13.89

2a

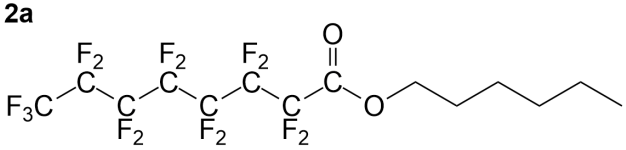

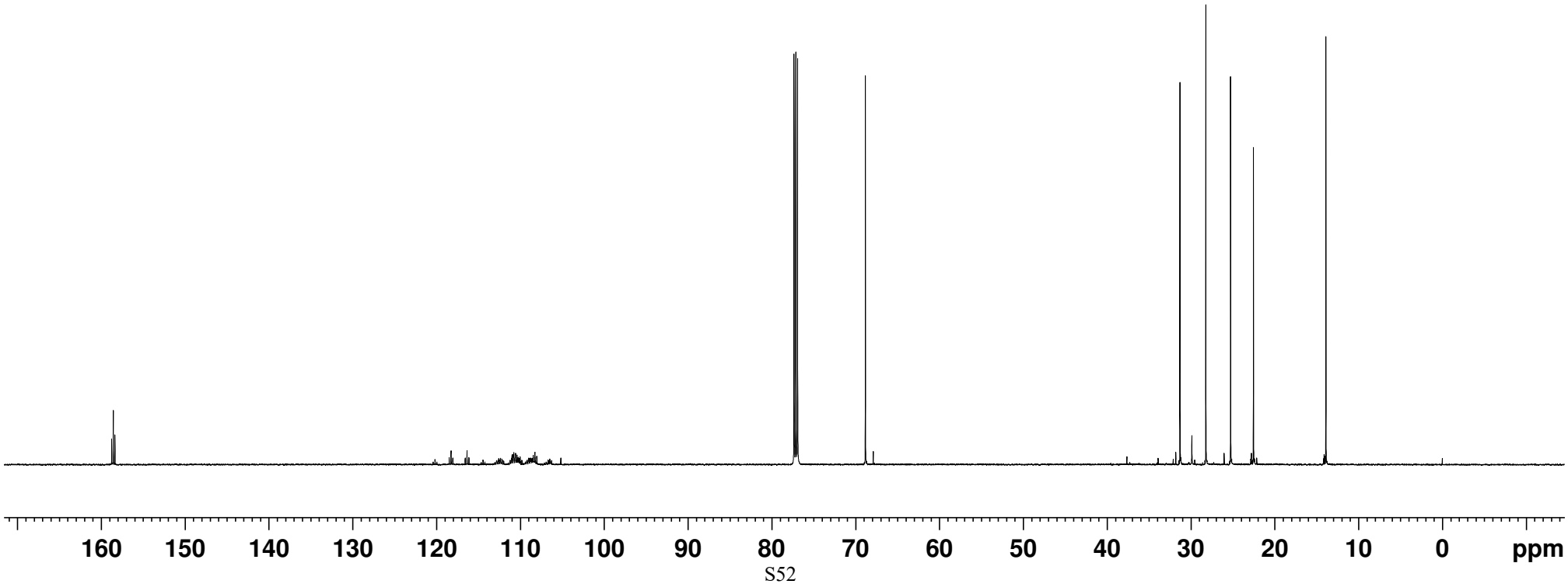

^{1}H NMR Spectrum

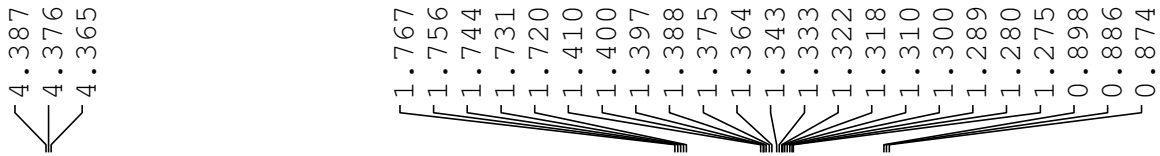

2b

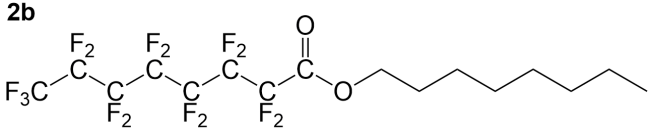

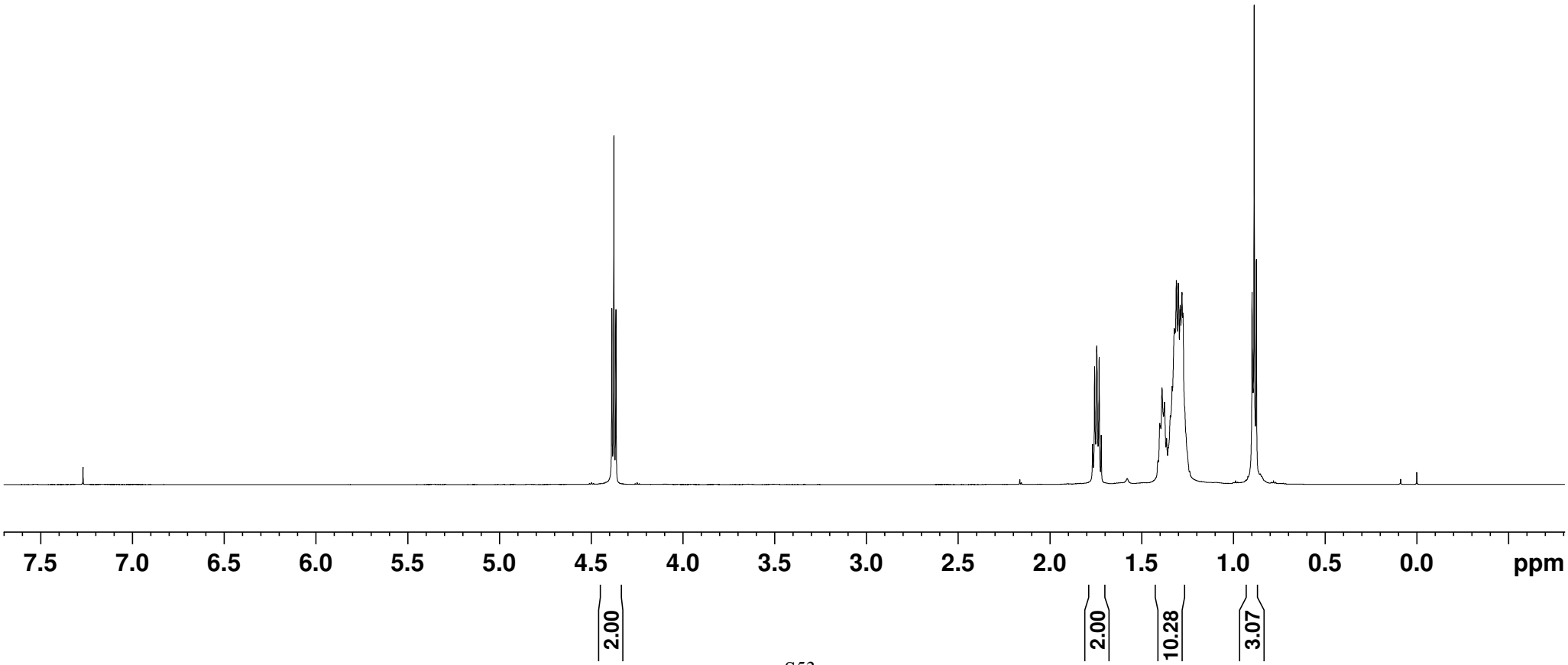

^{19}F NMR Spectrum

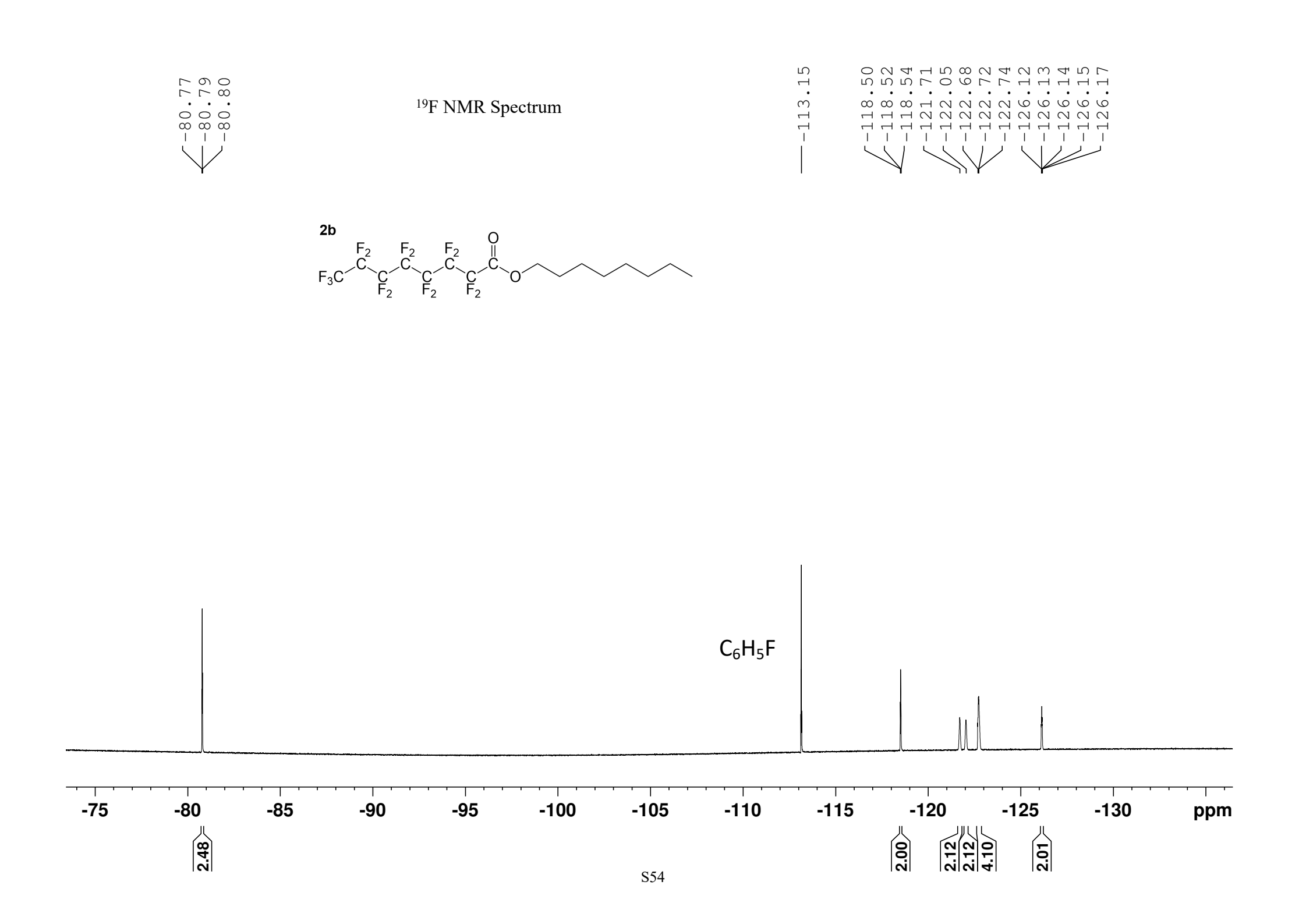

$^{13}C\{^{1}H\}$ NMR Spectrum

158.80
158.60
158.41

68.84

31.90
29.26
29.17
28.30
25.65
22.77

14.03

2b

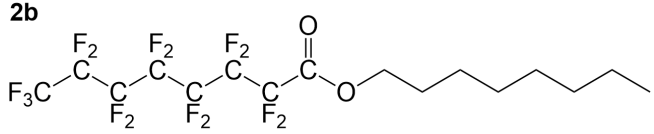

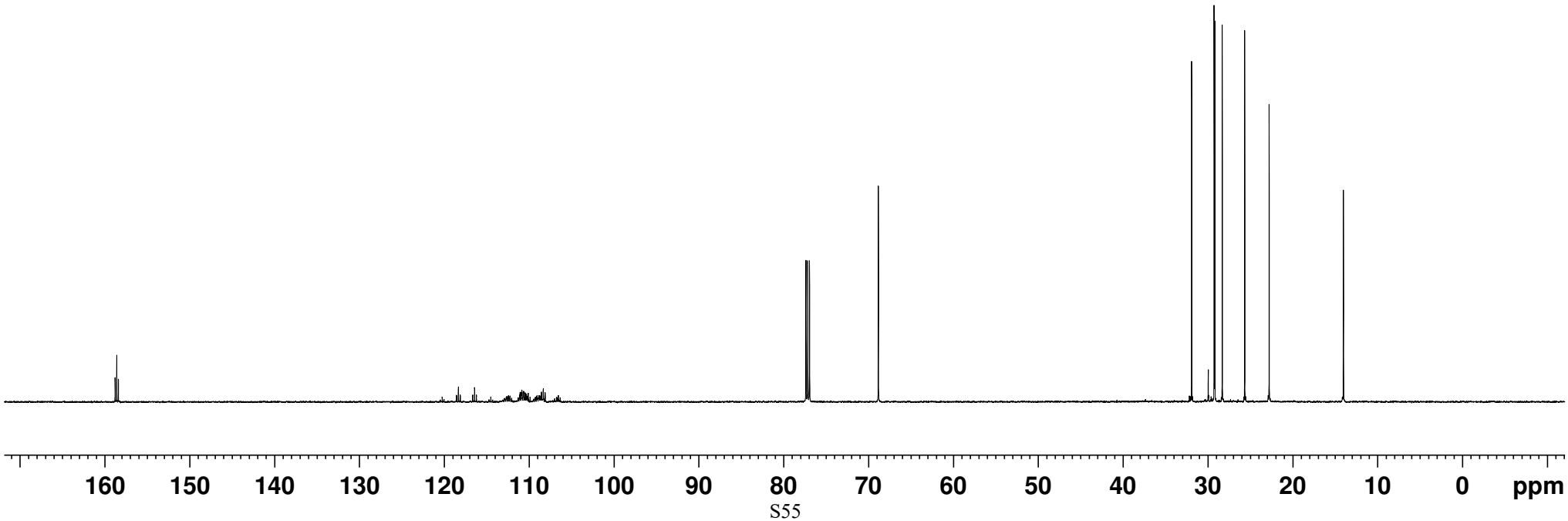

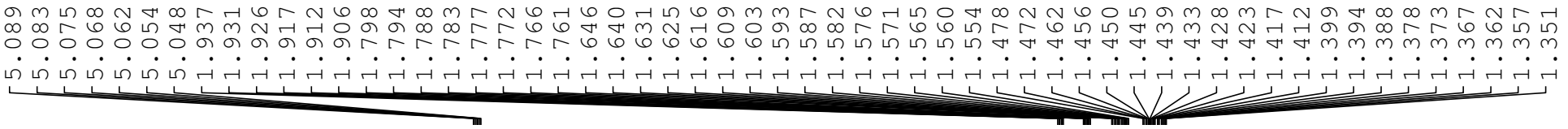

^{1}H NMR Spectrum

2c

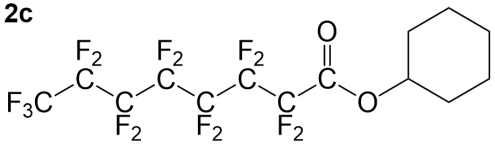

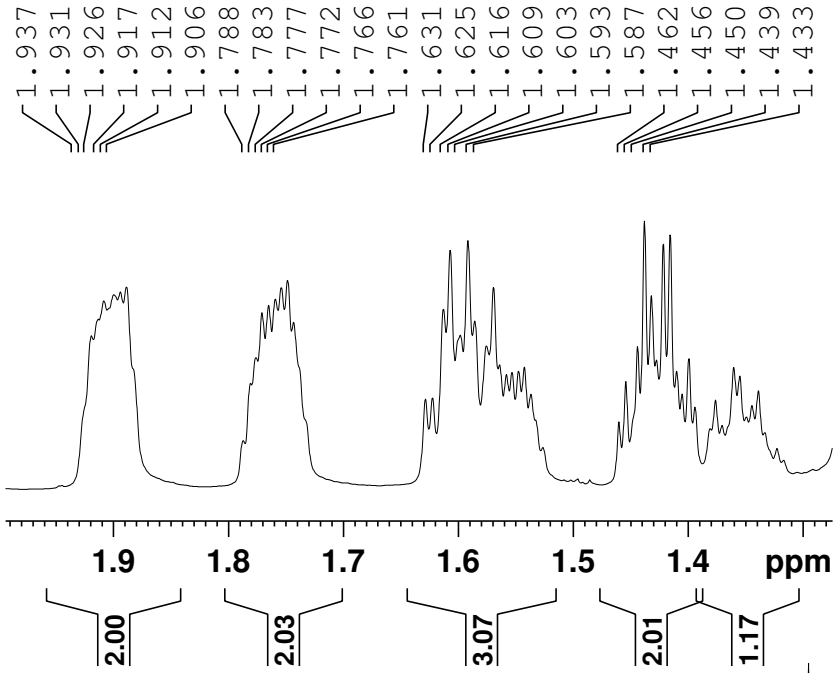

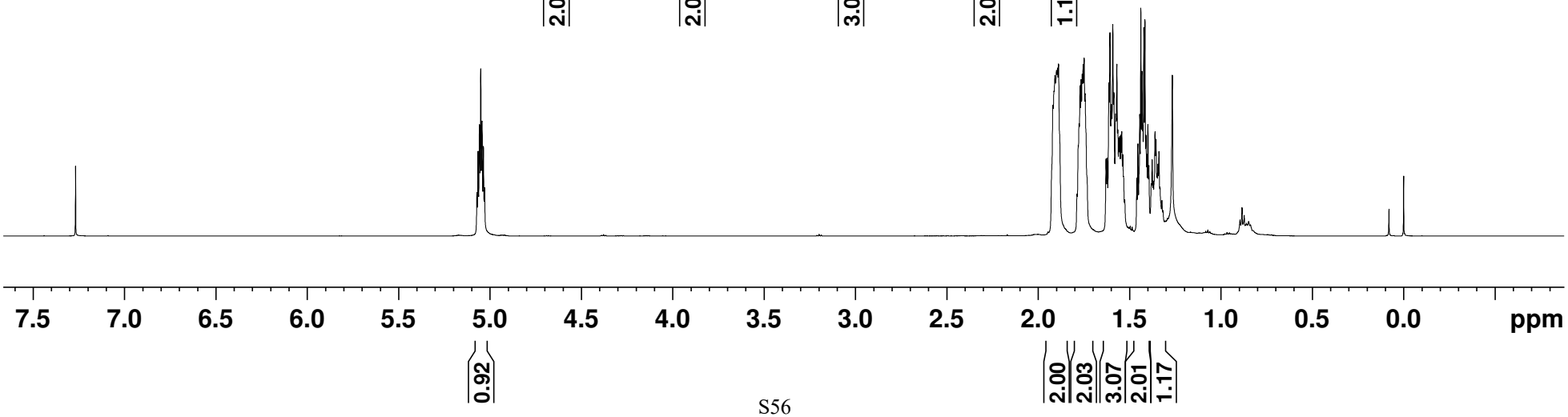

^{19}F NMR Spectrum

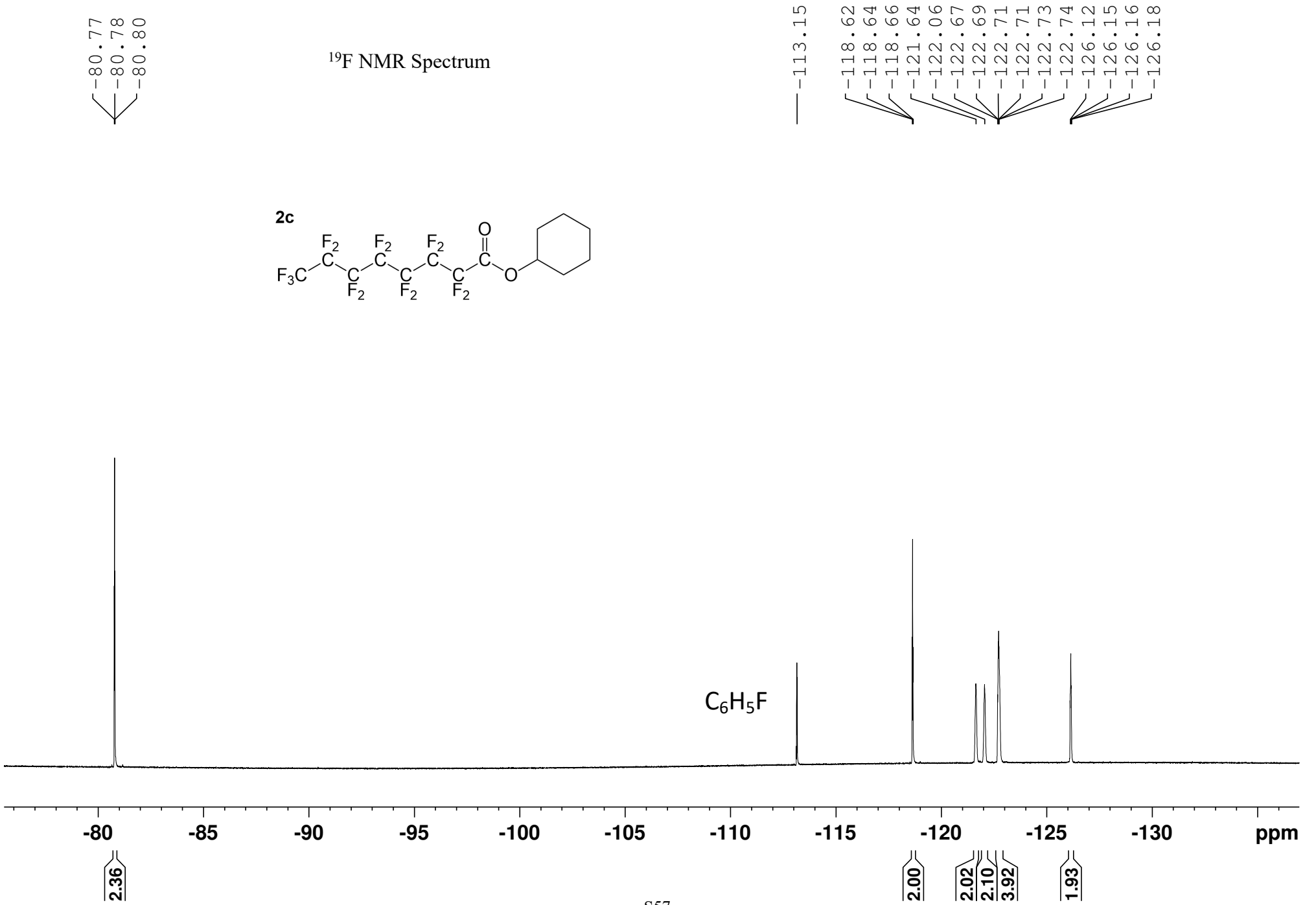

$^{13}C\{^{1}H\}$ NMR Spectrum

158.11
157.92
157.72
78.16
31.02
25.16
23.28

2c

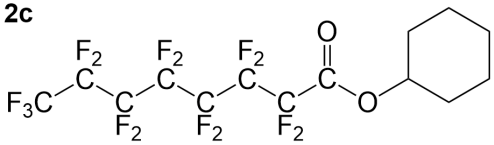

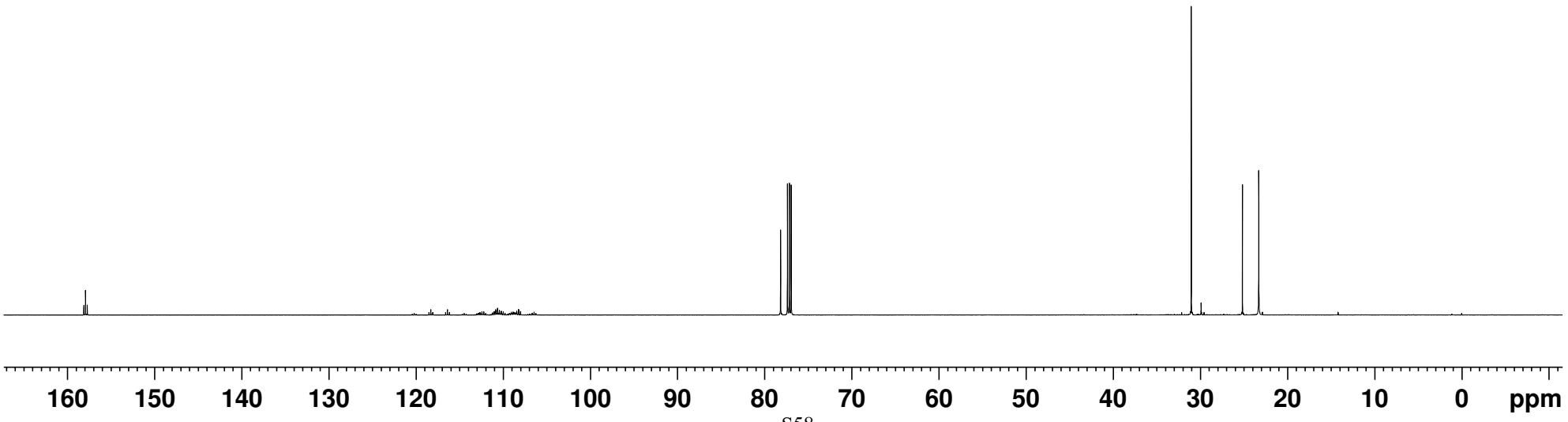

^{1}H NMR Spectrum

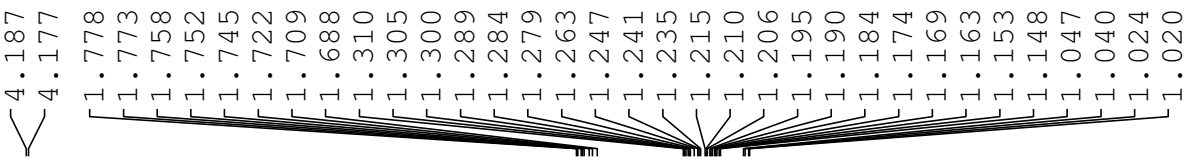

2d

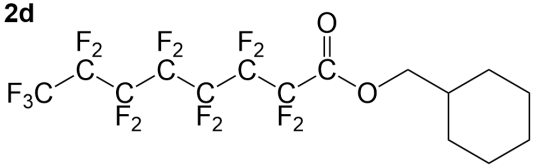

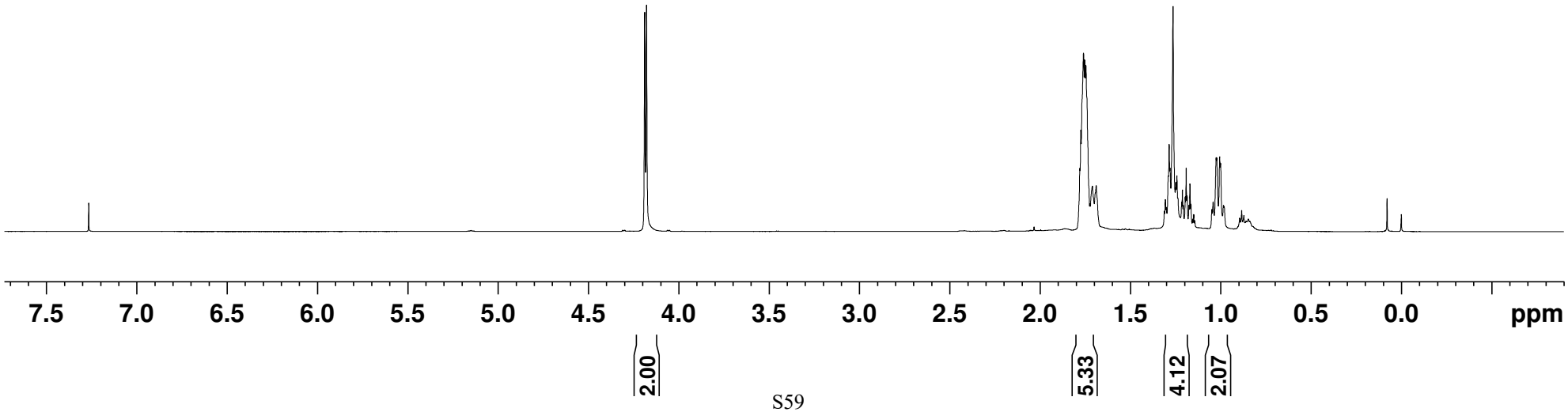

^{19}F NMR Spectrum

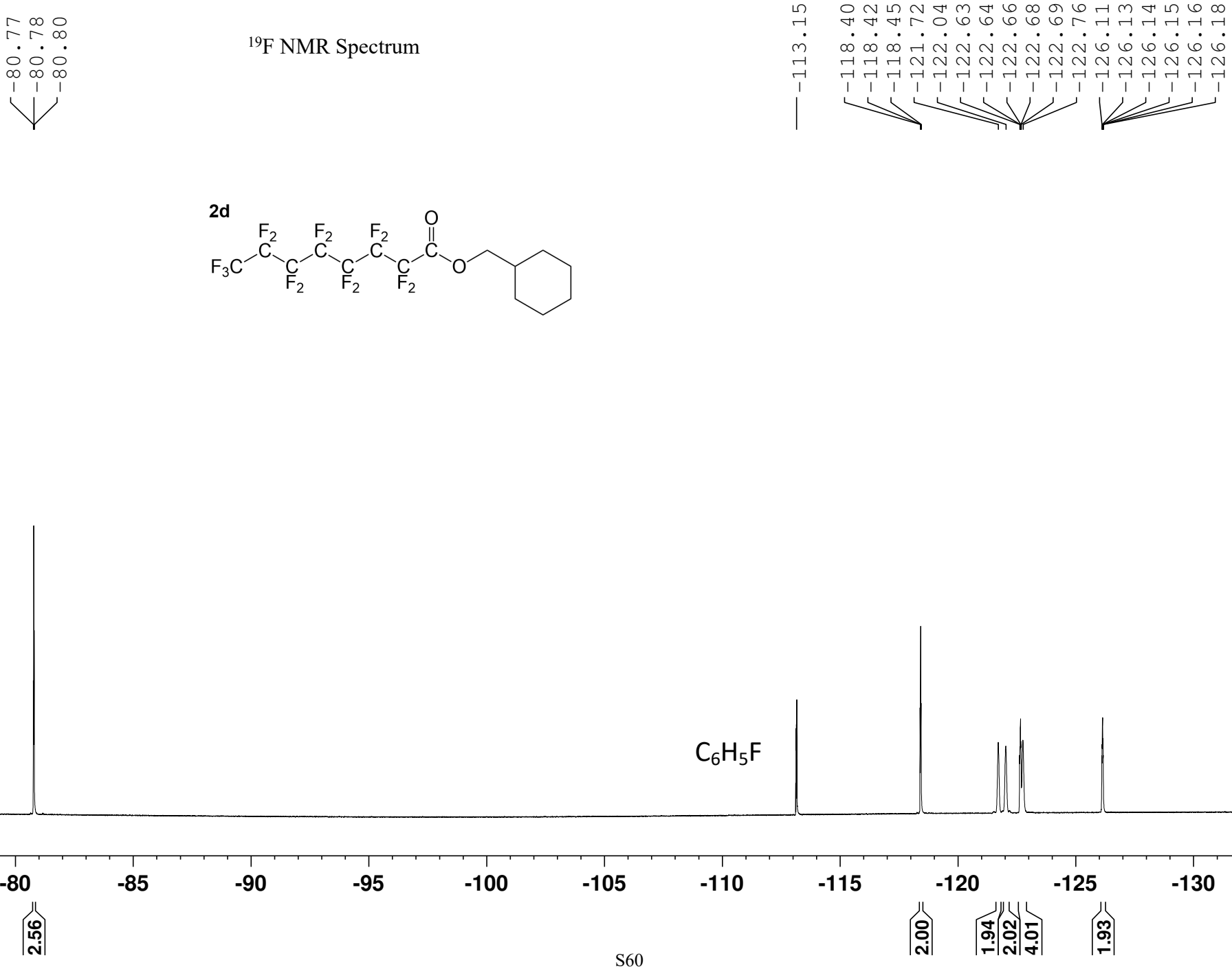

$^{13}C\{^{1}H\}$ NMR Spectrum

158.73
158.54
158.35
73.52
36.89
29.27
26.21
25.56

2d

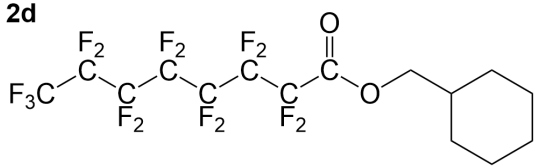

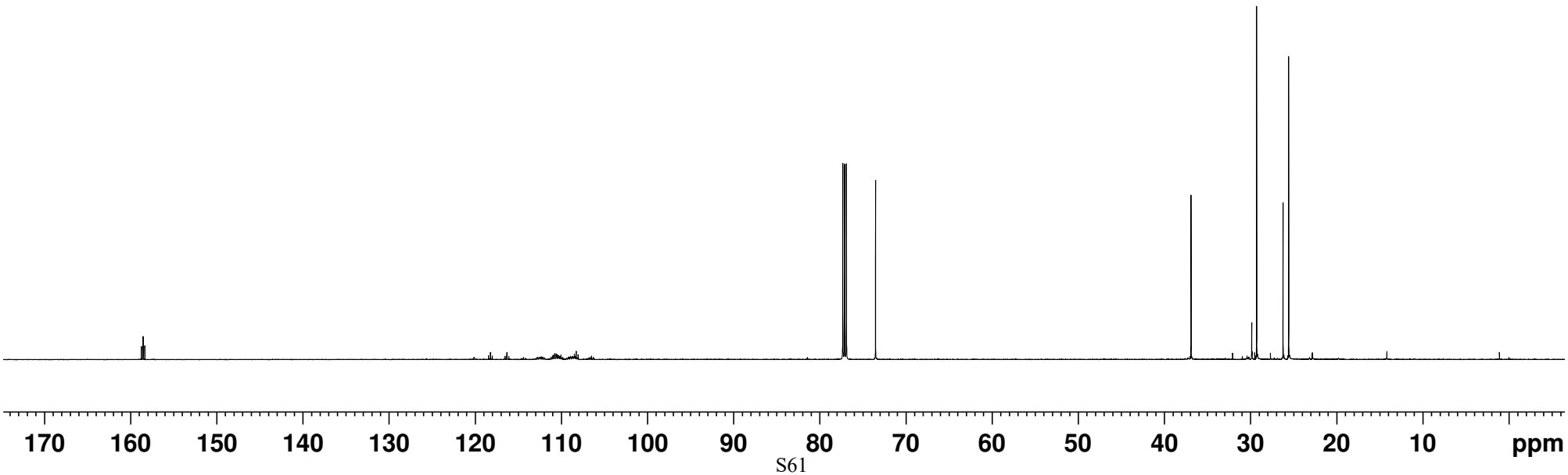

^{1}H NMR Spectrum

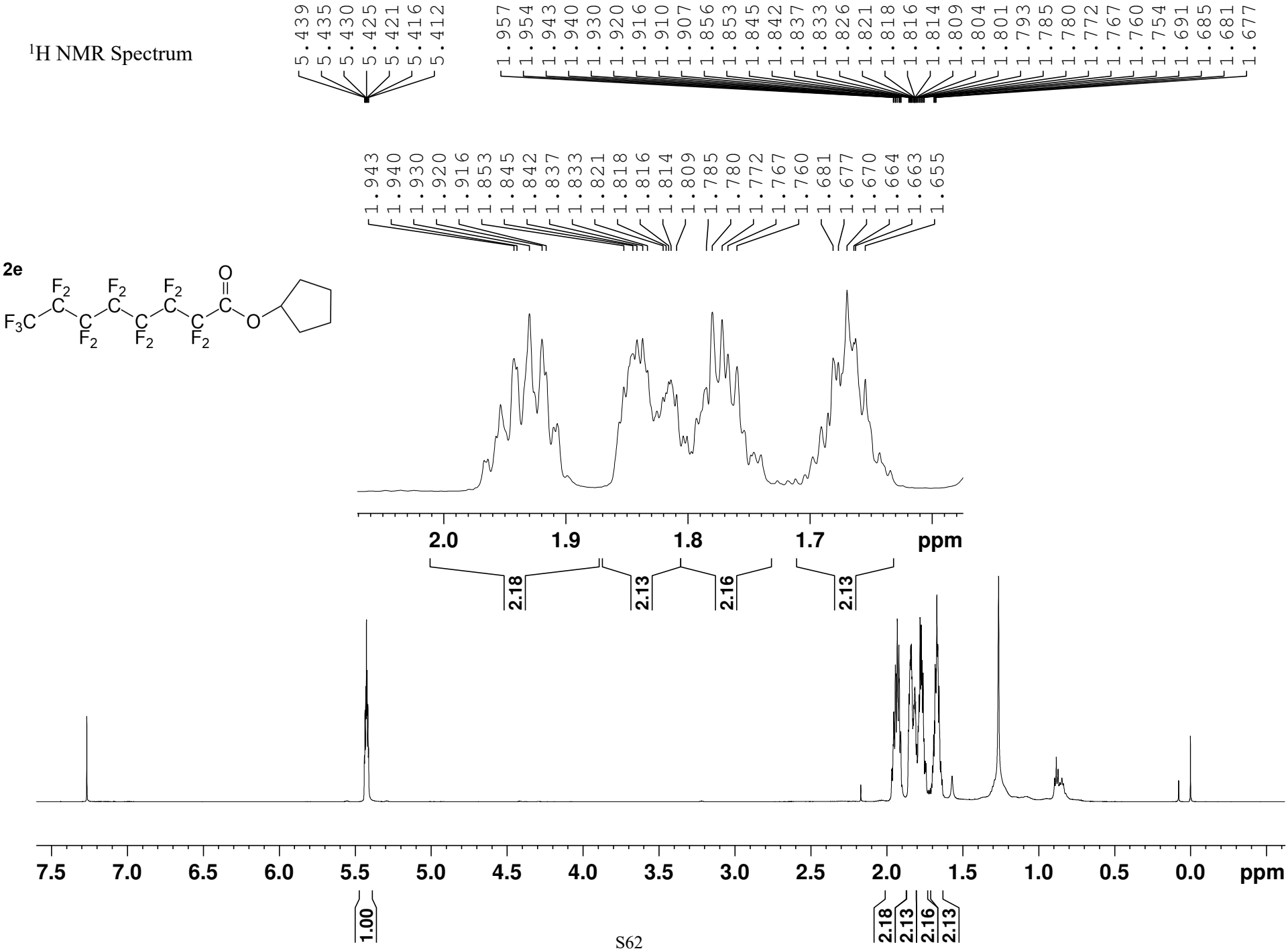

^{19}F NMR Spectrum

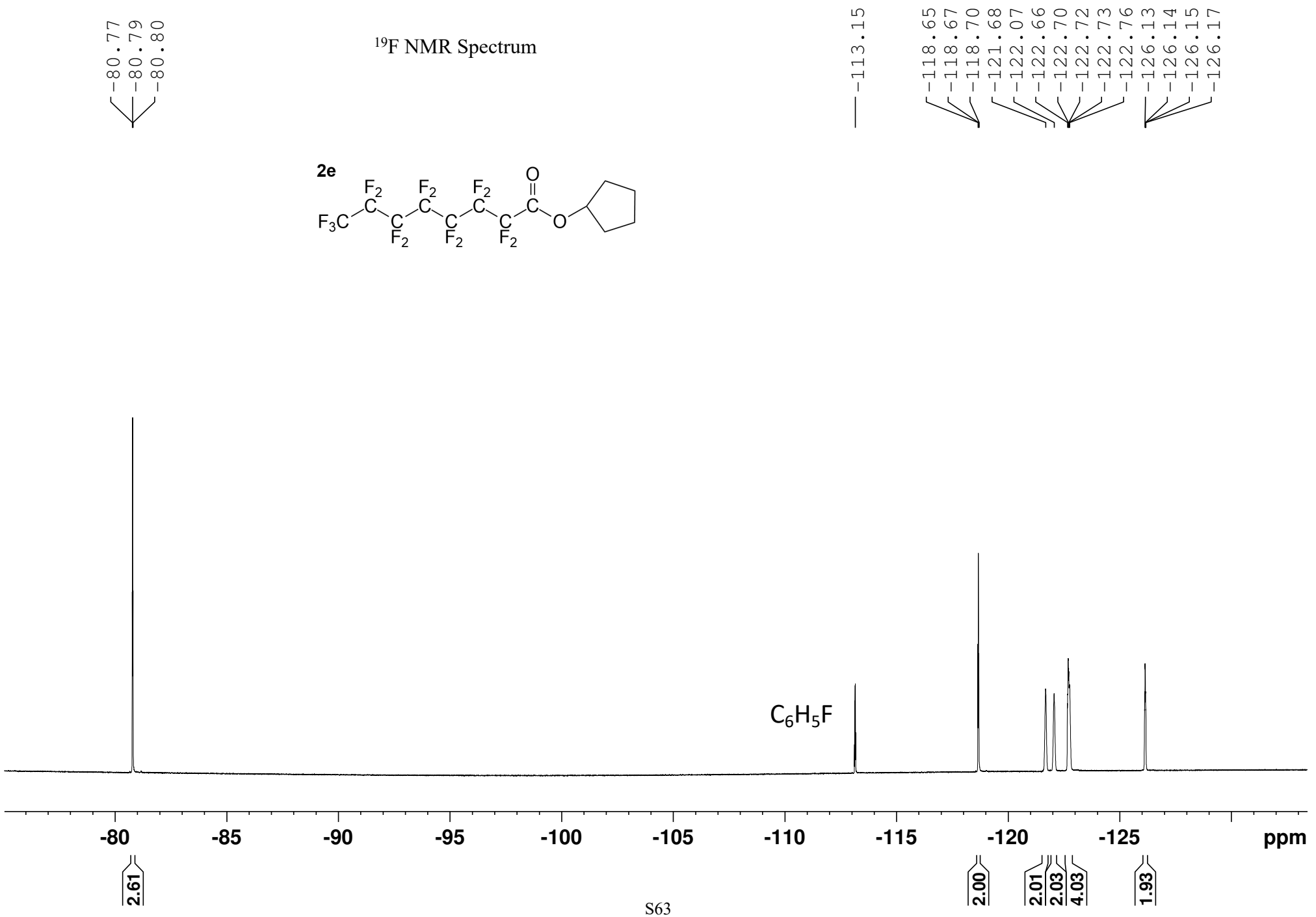

$^{13}C\{^{1}H\}$ NMR Spectrum

158.32
158.12
157.93
82.69
32.55
23.51

2e

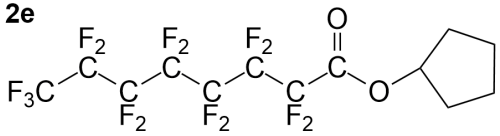

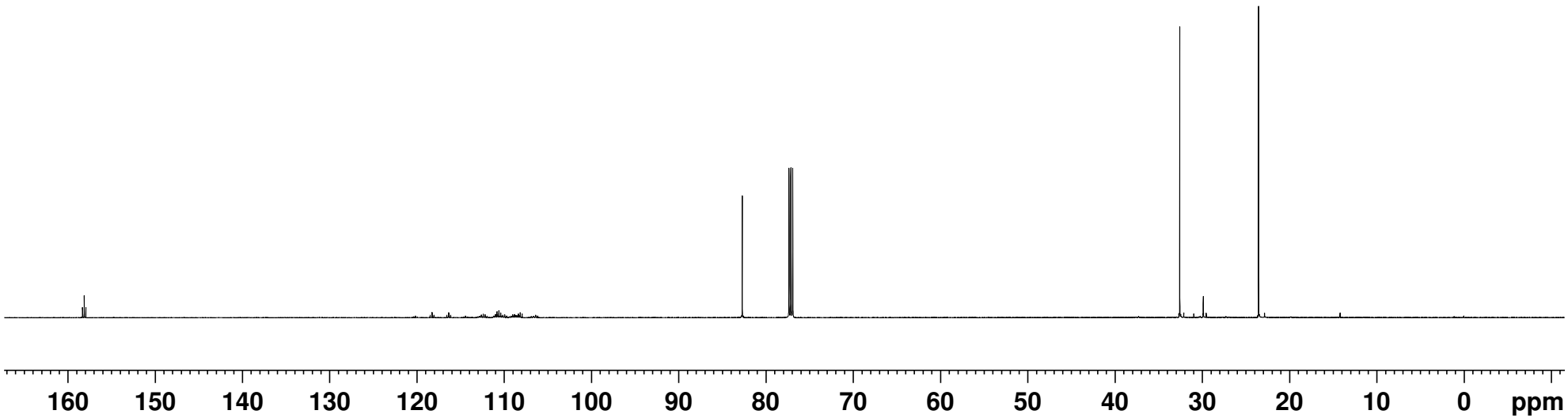

7.295
7.293
7.282
7.270
7.204
7.193
7.181
7.168
7.156

4.385
4.381
4.375
4.365

2.669
2.665
2.656
2.645
1.780
1.770
1.759
1.744
1.731
1.726
1.719
1.705

^{1}H NMR Spectrum

2f

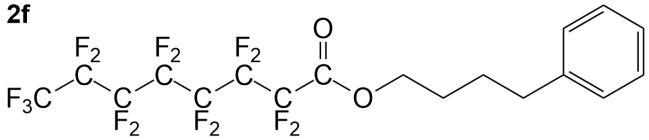

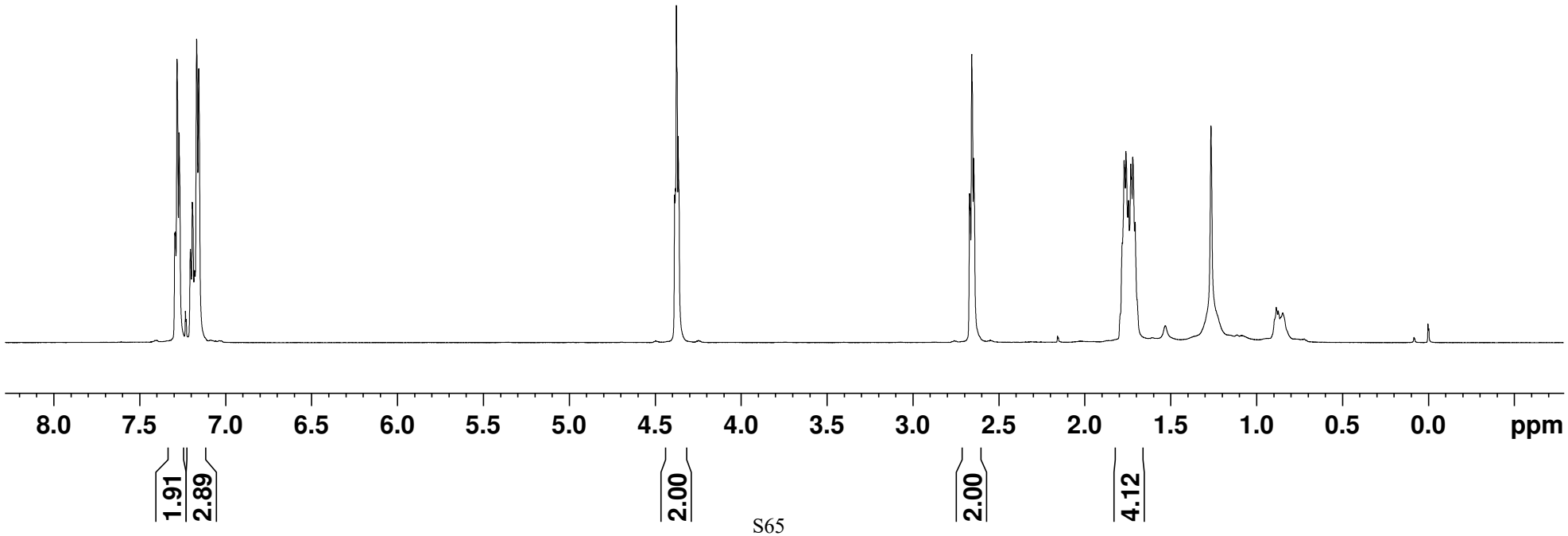

^{19}F NMR Spectrum

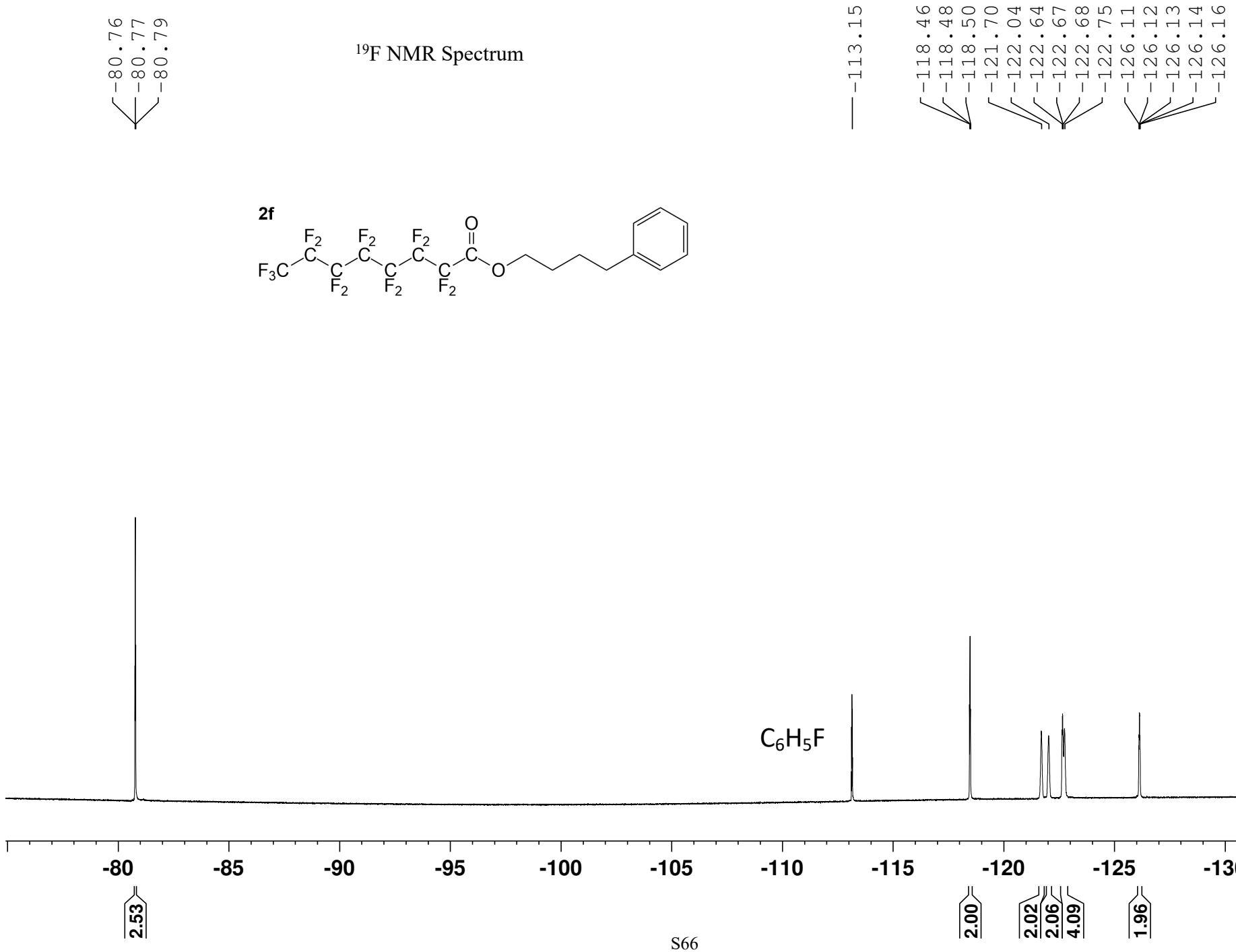

158.69
158.49
158.30
141.58
128.55
128.45
126.15

$^{13}C\{^{1}H\}$ NMR Spectrum

68.52
35.29
29.85
27.76
27.29

2f

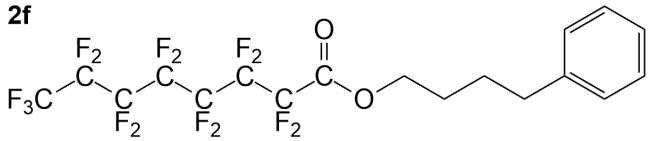

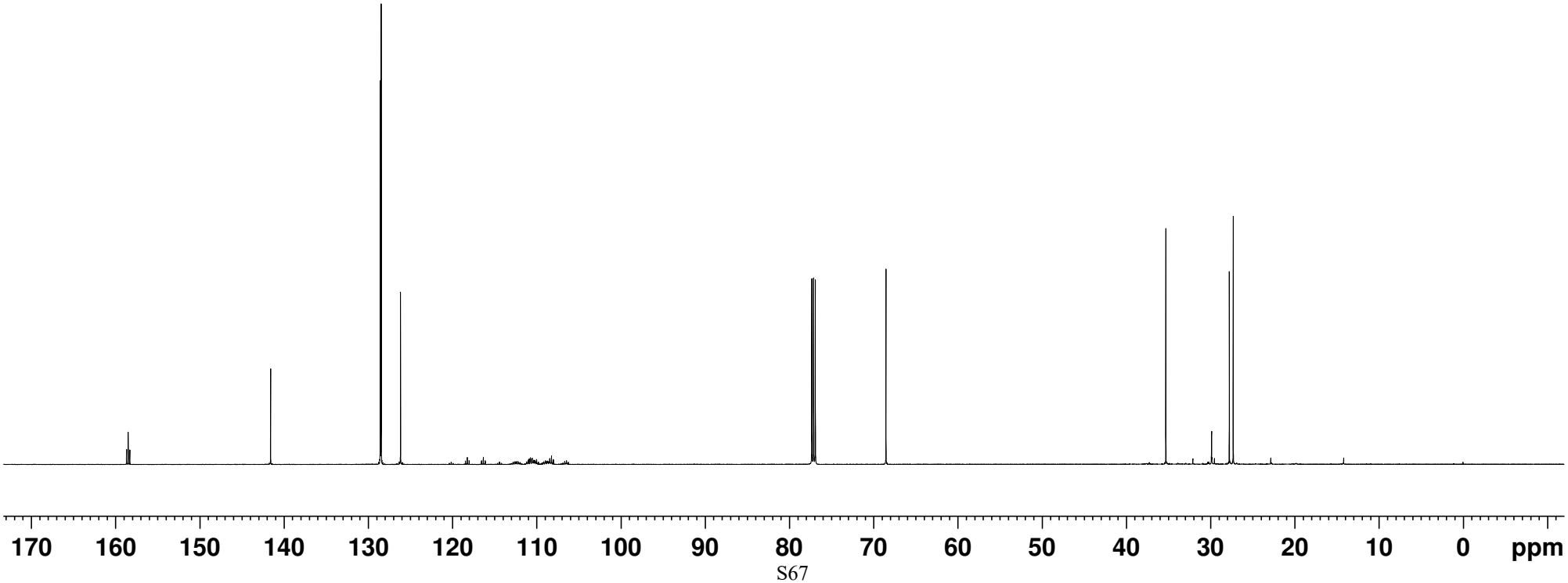

^{1}H NMR Spectrum

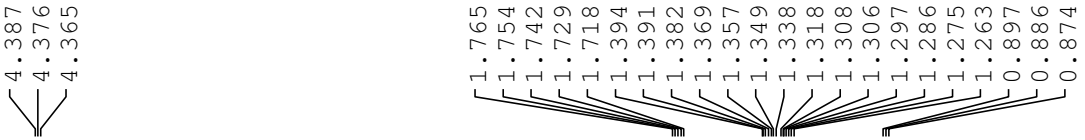

2g

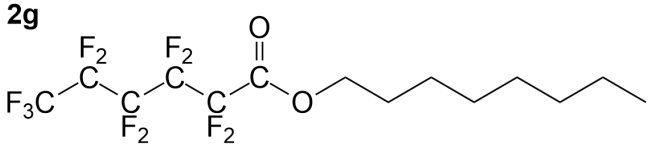

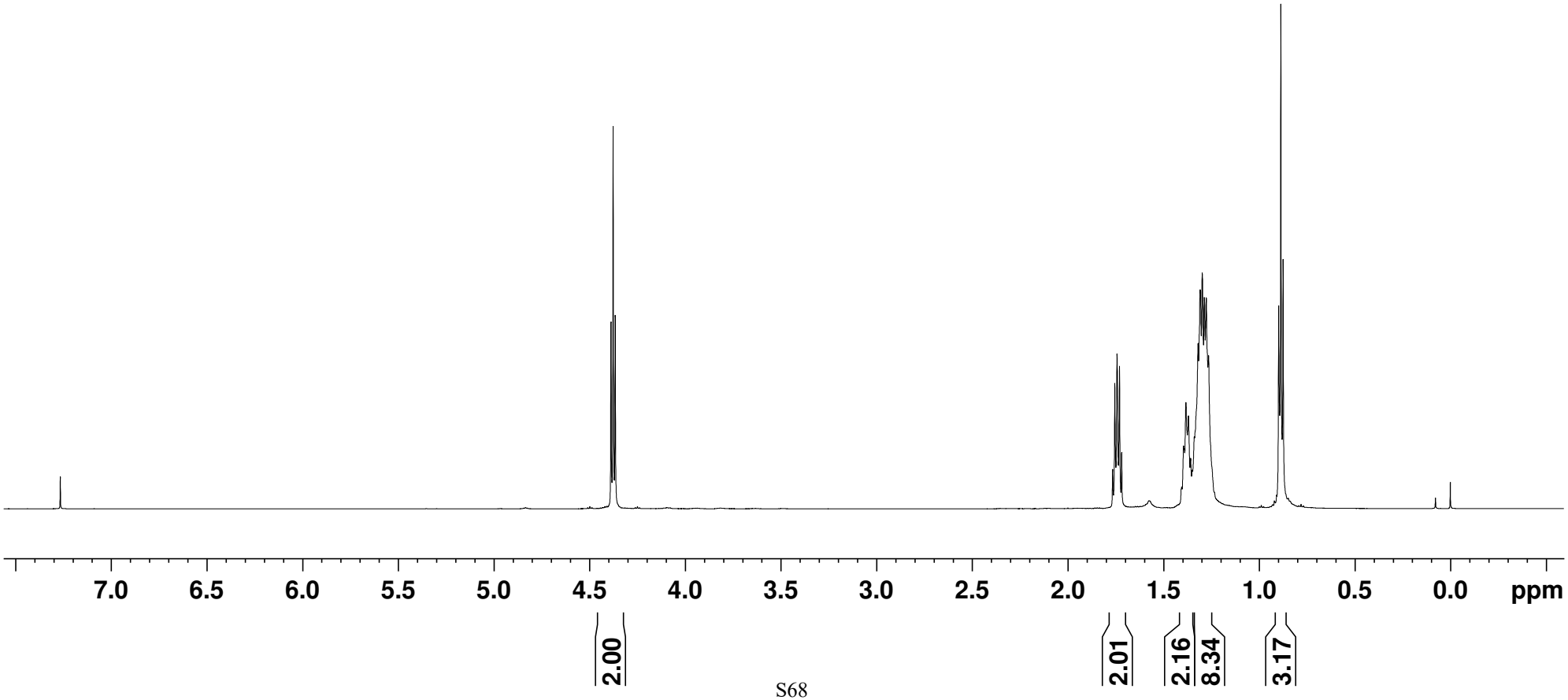

^{19}F NMR Spectrum

2g

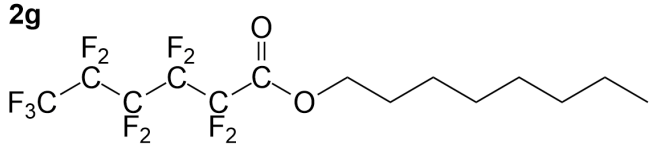

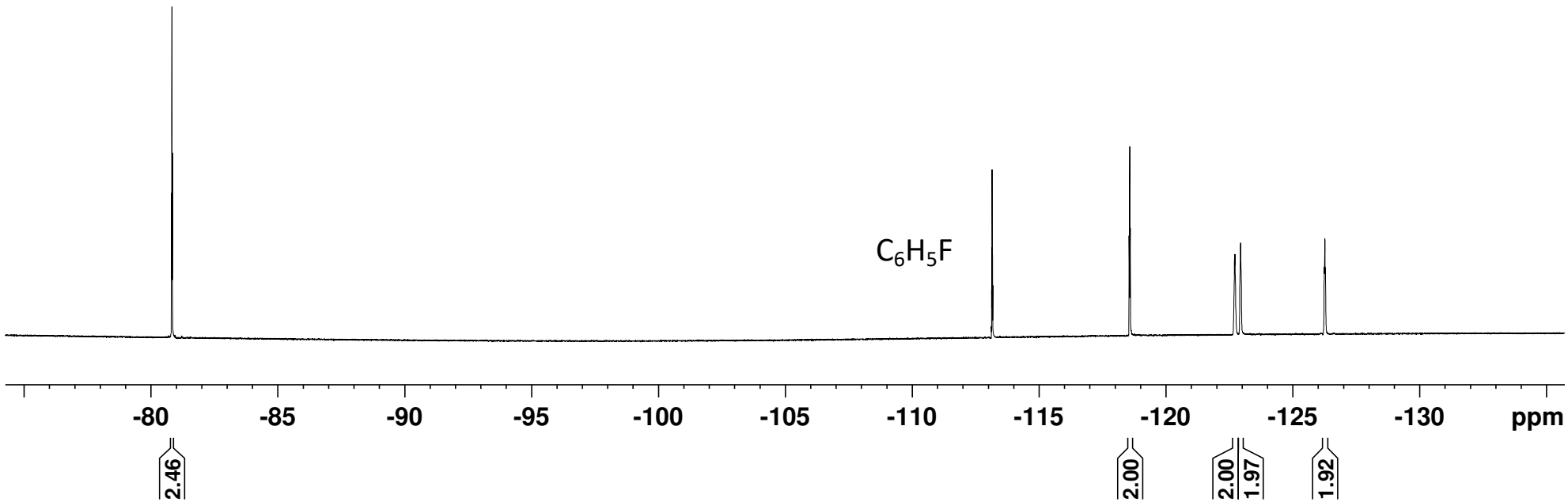

$^{13}C\{^{1}H\}$ NMR Spectrum

158.71
158.52
158.32

68.83

31.82
29.17
29.08
28.22
25.57
22.71

14.07

2g

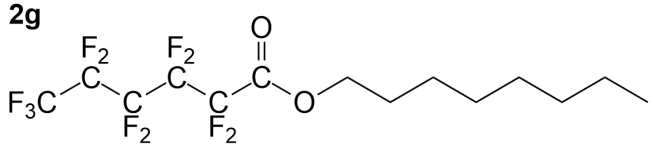

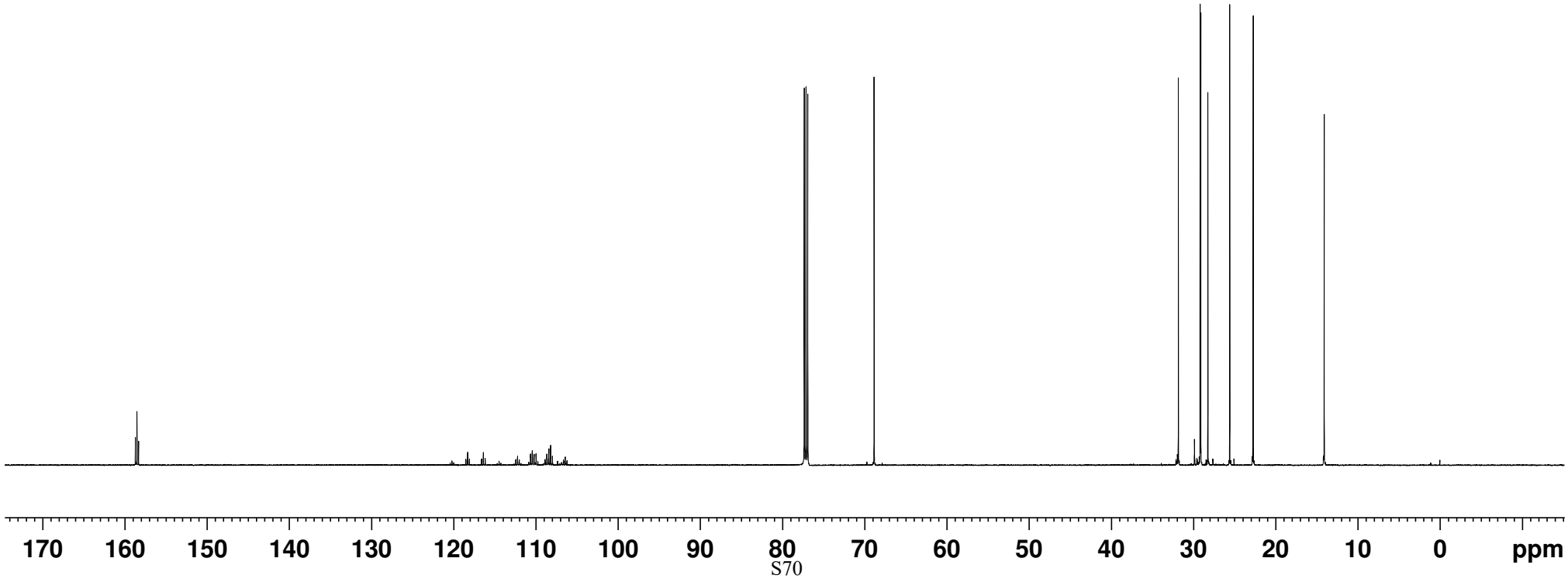

6. References

1 C.-C. Ko, L. T.-L. Lo, C.-O. Ng and S.-M. Yiu, *Chem. Eur. J.,* 2010, **16**, 13773.

2 (a) S. Sprouse, K. A. King, P. J. Spellane and R. J. Watts, *J. Am. Chem. Soc.,* 1984, **106**, 6647; (b) A. B. Tamayo, B. D. Alleyne, P. I. Djurovich, S. Lamansky, I. Tsyba, N. N. Ho, R. Bau and M. E. Thompson, *J. Am. Chem. Soc.,* 2003, **125**, 7377.

3 M. J. Frisch, G. M. Trucks and H.B. Schlegel, *Gaussian 09*, Revision B.01; Gaussian, Inc.: Wallingford, CT, 2009.

4 (a) C. Lee, W. Yang and R. G. Parr, *Phys. Rev. B: Condens. Matter Mater. Phys.,* 1988, **37**, 785; (b) A. D. Becke, *J. Chem. Phys.,* 1993, **98**, 5648.

5 P. J. Hay and W. R. Wadt, *J. Chem. Phys.,* 1985, **82**, 299.

6 G. Scalmani and M. J. Frisch, *J. Chem. Phys.,* 2010, **132**, 114110.